



Disks in Nearby Young Stellar Associations Found Via Virtual Reality

Susan Higashio^{1,2} , Marc J. Kuchner¹ , Steven M. Silverberg³ , Matthew A. Brandt⁴, Thomas G. Grubb⁴, Jonathan Gagné^{5,6} , John H. Debes⁷ , Joshua Schlieder¹ , John P. Wisniewski⁸ , Stewart Slocum⁹ , Alissa S. Bans¹⁰ , Shambo Bhattacharjee¹¹ , Joseph R. Biggs¹² , Milton K. D. Bosch¹² , Tadeas Cernohous¹² , Katharina Doll¹² , Hugo A. Durantini Luca^{12,13} , Alexandru Enachioaie¹² , Phillip Griffith, Sr.¹², Joshua Hamilton¹², Jonathan Holden¹² , Michiharu Hyogo^{12,14} , Dawoon Jung¹², Lily Lau¹², Fernanda Piñeiro¹², Art Piipuu¹², and Lisa Stiller¹²

The Disk Detective Collaboration

¹ NASA Goddard Space Flight Center, Exoplanets and Stellar Astrophysics Laboratory, Code 667, Greenbelt, MD 20771, USA; susan.higashio@gmail.com

² Center for Research and Exploration in Space Science and Technology, NASA/GSFC, Greenbelt, MD 20771, USA

³ MIT Kavli Institute, USA

⁴ NASA Goddard Space Flight Center, Science Data Processing Branch, Code 587, Greenbelt, MD, 20771, USA

⁵ Planétarium Rio Tinto Alcan, Espace pour la Vie, 4801 av. Pierre-de Coubertin, Montréal, Québec, Canada

⁶ Institute for Research on Exoplanets, Université de Montréal, Département de Physique, C.P. 6128 Succ. Centre-ville, Montréal, QC H3C 3J7, Canada

⁷ Space Telescope Science Institute, 3700 San Martin Dr., Baltimore, MD 21218, USA

⁸ Homer L. Dodge Department of Physics and Astronomy, University of Oklahoma, 440 W. Brooks Street, Norman, OK 73019, USA

⁹ Department of Computer Science, Johns Hopkins University, USA

¹⁰ Department of Physics, Emory University, 201 Dowman Drive, Atlanta, GA 30322, USA

¹¹ French National Centre for Scientific Research, 3 Rue Michel Ange, 75016 Paris, France

¹² Disk Detective Citizen Scientist

¹³ IATE-OAC, Universidad Nacional de Córdoba-CONICET. Laprida 854, X5000 BGR, Córdoba, Argentina

¹⁴ Meisei University, 2-1-1 Hodokubo, Hino, Tokyo 191-0042, Japan

Received 2021 December 8; revised 2022 March 17; accepted 2022 April 4; published 2022 June 28

Abstract

The Disk Detective citizen science project recently released a new catalog of disk candidates found by visual inspection of images from NASA’s Wide-field Infrared Survey Explorer mission and other surveys. We applied this new catalog of well-vetted disk candidates to search for new members of nearby young stellar associations (YSAs) using a novel technique based on Gaia data and virtual reality (VR). We examined AB Doradus, Argus, β Pictoris, Carina, Columba, Octans-Near, Tucana–Horologium, and TW Hya by displaying them in VR together with other nearby stars, color coded to show infrared excesses found via Disk Detective. Using this method allows us to find new association members in mass regimes where isochrones are degenerate. We propose 10 new YSA members with infrared excesses: three of AB Doradus (HD 44775, HD 40540 and HD 44510), one of β Pictoris (HD 198472), two of Octans-Near (HD 157165 and BD+35 2953), and four disk-hosting members of a combined population of Carina, Columba, and Tucana–Horologium: CPD-57 937, HD 274311, HD 41992, and WISEA J092521.90-673224.8. This last object (J0925) appears to be an extreme debris disk with a fractional infrared luminosity of 3.7×10^{-2} . We also propose two new members of AB Doradus that do not show infrared excesses: TYC 6518-1857-1 and CPD-25 1292. We find HD 15115 appears to be a member of Tucana–Horologium rather than β Pictoris. We advocate for membership in Columba–Carina of HD 30447, CPD-35 525, and HD 35841. Finally, we propose that three M dwarfs, previously considered members of Tucana–Horologium are better considered a separate association, tentatively called “Smethells 165”.

Unified Astronomy Thesaurus concepts: Debris disks (363); Moving clusters (1076); Infrared excess (788)

1. Introduction

Stars in young moving groups and associations often show excess emission at infrared (IR) wavelengths pointing to the presence of circumstellar disks (e.g., Zuckerman et al. 2011; Boucher et al. 2016; Moór et al. 2016): gas-rich protoplanetary and transitional disks, and gas-poor debris disks. As membership in these young moving groups and associations yields stellar age estimates, these disks in young moving groups have become central to our understanding of planet formation. They provide us with a timeline for disk evolution between ~ 3 and 200 Myr, chronicling the transition from primordial and debris

stages, and providing critical time constraints for gas and planetesimal accretion and orbit evolution (e.g., Mamajek 2009; Meng et al. 2017). Furthermore, many disks with resolved images, like β Pictoris, HR 4796A, AU Microscopii, belong to young moving groups; knowing the ages of these disks allows us to examine and model their dynamics in detail (e.g., Nesvold & Kuchner 2015a, 2015b; Grady et al. 2020; Moór et al. 2020).

Thanks to recent releases of data from the European Space Agency’s (ESA) Gaia telescope, Data Release 2 (DR2) and Early Data Release 3 (EDR3), there has been a flurry of activity to identify new young stellar association (YSA) candidates. Some of these studies used infrared excess as a clue to group membership, and others used Gaia-informed group membership as a way to find new disks. For example, Esplin et al. (2018) announced 179 new disks in the Upper Scorpius Association based on Gaia data and photometry from NASA’s Wide-field Infrared Survey Explorer (WISE) mission.



Original content from this work may be used under the terms of the [Creative Commons Attribution 4.0 licence](https://creativecommons.org/licenses/by/4.0/). Any further distribution of this work must maintain attribution to the author(s) and the title of the work, journal citation and DOI.

Luhman & Esplin (2020) refined this work using DR2 astrometry. Melton (2020) identified 27 candidate members of the Lupus star-forming region by combining DR2 data with disk determinations based on photometry from NASA’s Spitzer Space Telescope. Zuckerman et al. (2019) described the large percentage of M-type stars with warm excess infrared emission in the χ^1 Fornacis cluster. Zuckerman (2019) argued for the validity of the nearby Argus association based in part on a membership list containing 80% infrared-excess stars.

Nonetheless, much more remains to be learned about disks in moving groups using Gaia data, especially in concert with infrared photometry from WISE. The presence of a disk can be an especially vital youth indicator for A- and F-type stars, a mass range where isochrones can be degenerate, and Lithium depletion methods for age assessment fail.

The Disk Detective citizen science project (Kuchner et al. 2016), launched in 2014, asked members of the public to examine images of WISE sources to search for reliable disk candidates: stars with infrared excess at $22\ \mu\text{m}$. This effort has generated a catalog of roughly 30,000 strong disk candidates, many of which are known to be YSA members. A representative subset of these sources has been checked for background objects via higher-resolution imaging (Silverberg et al. 2018). As possession of a disk is often a sign of youth (but see also the discussion on Be stars in Kuchner et al. 2016), this new catalog of reliable disk candidates has great potential as a source of new YSA members.

Indeed, we have begun combing the Disk Detective catalog to identify new members of nearby YSAs (including young moving groups), using Bayesian Analysis for Nearby Young AssociationNs (BANYAN Σ ; Gagné et al. 2018b; S. M. Silverberg et al. 2022, in preparation). As Gaia DR2 became available in April 2018, several codes and techniques for identifying new moving group candidates have seen wide use. The multivariate Gaussian model (Gagné et al. 2018b) known as BANYAN Σ uses a Bayesian algorithm to identify new YSA members. This tool calculates membership probabilities of stars for 27 YSAs within 150 pc of the Sun using multivariate Gaussian distributions in six dimensions, that is, the X, Y, Z, U, V, W space. The LocAtIng Constituent mEmbers In Nearby Groups (LACEwING) algorithm (Riedel et al. 2017b) uses a frequentist approach combined with triaxial ellipsoid models and optionally an epicyclic trace-back code. Additionally, Lee & Song (2019a) developed a new four-stage iterative method for evaluating the membership in nearby YSAs. The Lee & Song (2019a) paper contains 3D ellipsoidal models in XYZ and in UVW for nine moving groups that are younger than 200 Myr and within 100 pc of the Sun.

These tools have greatly streamlined the process of finding new candidate members of YSAs for most situations. However, all of the tools described above, including BANYAN Σ , are limited by the quality of their YSA models—e.g., the parameters of their triaxial ellipsoids. The quality of these models is in turn determined by the number and fidelity of the lists of assumed bona fide members of each YSA. Since our process had the potential to add multiple new members to each moving group, and as Gaia represents such a dramatic shift in the quantity and quality of astrometric data for nearby stars, we sought an alternative, ab initio process for identifying new YSA members that would not rely on such pre-Gaia membership lists.

This paper describes our novel VR-based approach and the new candidate YSA members we have identified. We describe

the Disk Detective citizen science project and the new database of disk candidates available in the Mikulski Archive for Space Telescopes (MAST) in Section 2. We discuss the VR methodology in Section 3. We discuss the newly identified YSA members with disks in Sections 4, 5, and 6, with further discussion about WISEA J092521.90-673224.8 in Section 7.

2. The Disk Detective Citizen Science Project

The Disk Detective citizen science project, first launched in 2014 January, asks members of the public to examine images of sources from the AllWISE catalog to search for reliable disk candidates. Most objects that appear to have infrared excesses based on simple WISE color cuts are in fact false positives created by confusion or contamination (Kennedy & Wyatt 2012; Silverberg et al. 2018; Dennihy et al. 2020). Disk Detective solves this problem through citizen science; volunteers at Disk Detective have worked to weed out most of the false positives by examining images of source from the AllWISE catalog, the 2MASS project, the Sloan Digital Sky Survey and the Digitized Sky Survey (DSS; Silverberg et al. 2018).

The Disk Detective project has resulted in several noteworthy discoveries, including a new category of disks, the “Peter Pan Disks” (Silverberg et al. 2016, 2020; Coleman & Haworth 2020; Lee et al. 2020). Peter Pan disks are so called because the stellar ages, based on moving group membership, indicate that these gas-rich disks have lasted far longer than the typical lifetimes assumed for such disks. Disk Detective citizen scientists discovered the first example of this phenomenon (Silverberg et al. 2016; Murphy et al. 2018) and several later examples (Silverberg et al. 2020). The Disk Detective project discovered the closest brown dwarf disk younger than 10 Myr (Schutte et al. 2020) and 12 likely warm dust disks around candidate members of co-moving pairs based on Gaia astrometry (Silverberg et al. 2018), which supports the hypothesis that warm dust is associated with binary systems (Zuckerman 2015). Disk Detective citizen scientists also helped locate the oldest known disk around a white dwarf (Debes et al. 2019) and the first debris disk discovered around a star with a white dwarf companion (Kuchner et al. 2016). Fifteen citizen scientists have become named coauthors on refereed publications as a result of their participation in Disk Detective (not including this paper).

To extend Disk Detective information to those objects that were not fully classified before the project went offline on 2019 April 30, we used the objects that had been fully classified to train a GoogLeNet (Szegedy et al. 2014) neural network. The full details of this process will be presented in S. M. Silverberg et al. (2022, in preparation). Briefly, we composited the nine images used on the Disk Detective site for each subject into one image, along with the classification information for that subject, and used this to train the neural network. We tested three methods to determine whether a given subject was a good disk candidate: if “None of the above” was a simple majority of classifications (majGood), a plurality of classifications (pluralGood), or made up at least 20% of classifications (twentyGood). The neural network then assigned each new (unclassified) subject a score of 0–100 based on each of the above neural networks. We then asked four expert citizen scientists to blindly evaluate 476 subjects with a “good” score >90 out of 100 by the “majority”-trained neural network. Of these 476 subjects that were identified as likely good disk

candidates by the neural network, the citizen scientists found 118 to be false positives; i.e., 25% of the subjects classified as good by the neural network would not have been classified as “None of the Above/Good disk candidate” by citizen scientists. While this false-positive rate is nonnegligible, it is low enough to be useful for some purposes—e.g., searching for candidate members of YSAs. We added the subjects classified by the neural net (those with the `majGood` parameter >90) to the list of Disk Detective disk candidates we used in this paper. A catalog of Disk Detective data is available to the public in the MAST archive.¹⁵ This catalog contains all of the disk candidates we used, including those selected by the neural network.

3. Examining Young Stellar Associations Using Virtual Reality

We have been examining Gaia DR2 data on positions and velocities of stars using the PointCloudsVR application combined with the HTC Vive system. PointCloudsVR, available on GitHub at <https://github.com/nasa/PointCloudsVR>, leverages the advantages of virtual reality to intuitively immerse viewers in the 3D data and easily see spatial relationships. It uses two controllers to move around in and zoom/pan in and out of an interactive 360° scene. We used a custom application layer developed by the Augmented Reality/Virtual Reality (AR/VR) Research & Development Laboratory at NASA's Goddard Spaceflight Center (GSFC) to load and visualize the Gaia data, and animate the stars according to the space velocities measured by Gaia. This (AR/VR) Research & Development Laboratory has developed VR software for a variety of space science and engineering applications, including heliophysics and planetary science applications. VR in general has seen a variety of applications in astrophysics during the last few years, including displaying Ly α maps (Lee et al. 2018), mapping the morphology of a molecular cloud (Romano et al. 2019) and cataloging galaxy groups (Lambert et al. 2020).

Of the 1.7 billion stars in DR2 (Gaia Collaboration et al. 2018), approximately 4 million stars have both Gaia-measured radial velocities and Gaia-measured parallaxes greater than 0.6. We loaded this sample into the PointCloudsVR app. We also loaded lists of the Gaia IDs of members of 40 YSAs from the literature (see below).

We then loaded the Gaia IDs of our catalog of 48,965 disk candidates from Disk Detective, including 13,626 that were determined by the neural network, as described above. We used these lists to highlight and color code the representations of the Gaia DR2 stars in our VR simulations. For example, in one run all the stars with disk candidates from Disk Detective were color coded orange, and all the known members of the Tuc-Hor association green, and turned off all the rest of the Gaia DR2 catalog. Figure 1 shows a representative screenshot of the PointCloudsVR simulation—collapsed to two dimensions of course. We used this color coding to highlight various lists of stars to search for new YSA members, one YSA at a time, using the following iterative process.

First, we highlighted the members of the YSA, observed them from various angles and distances to get a sense of its distribution in the XYZ space, and evolved the stellar positions backward and forward in time to develop an intuition for the group's velocity distribution. Then we highlighted our disk

candidates alongside the known YSA members and compared them to look for possible new kinematic YSA members. Once we had recorded a preliminary list of the disk candidates associated with the YSA, we created a new catalog combining the new candidate members with the previously published members. We then highlighted only that new combined catalog, examined it, and removed any obvious interlopers. Then we repeated this process, highlighting the whole Disk Detective catalog again, comparing it with the new combined catalog to find new candidate members, again combining any new candidates and checking for interlopers. We repeated this inspection process for each YSA in our database until it stopped turning up new candidates.

Although numerical clustering algorithms can also be used to search for and scope out the size of these six-dimensional clumps, our VR approach has multiple advantages over clustering techniques. First, YSAs vary greatly in their degrees of clustering, and some of them have multiple components, such as a tight core combined with a more diffuse halo. The human eye has no difficulty recognizing these structures, which could easily fool a clustering algorithm unless it were repeatedly retuned. Second, Gaia detection limits impose a luminosity-dependent edge to any large structure on the side away from the Sun. A clustering algorithm would need to be taught about this effect, while a human eye recognizes it instinctively.

We worked our way through eight different YSAs using VR, comparing the Disk Detective catalog bit by bit against the lists of known YSA members. Table 1 lists all of the proposed new candidate YSA members with disks we found, and Table 2 lists co-movers and companions to the proposed new candidate YSA members with disks. Figures 2 through 14 show position/velocity and color–magnitude diagrams (CMDs) for each of the YSAs where we identified likely new members. The assumed members are plotted in blue, and the sources of each membership list appear in the figure captions. The proposed new members are plotted in red.

4. New Candidate YSA Members and YSA Members with Disks

Here we discuss each of the YSAs we examined except for Carina, Columba, and Tucana–Horologium. We will examine those three together in a subsequent section. We also briefly discuss each star of interest.

4.1. AB Doradus Moving Group

The closest known moving group, AB Doradus (AB Dor; Zuckerman et al. 2004), contains a core or nucleus of ~ 10 stars at a distance of 20 pc, along with dozens of purported “stream” members distributed across the sky. Figure 2 shows a list of known members of AB Doradus from Lee & Song (2019a). Several groups have recently proposed membership lists for this group, including Gagné et al. (2018b), Gagné et al. (2018c), Gagné & Faherty (2018), and Schneider et al. (2019). The new, more comprehensive, list by Lee & Song (2019a) utilizes Gaia DR2 and machine learning.

In this figure, the origin of each arrow is the star's current Galactic position from Gaia DR2. The arrows show how far each star moves in 1000 yr based on its Gaia DR2 velocity. Based on the findings by Gagné et al. (2018a) the age of AB

¹⁵ <https://mast.stsci.edu>

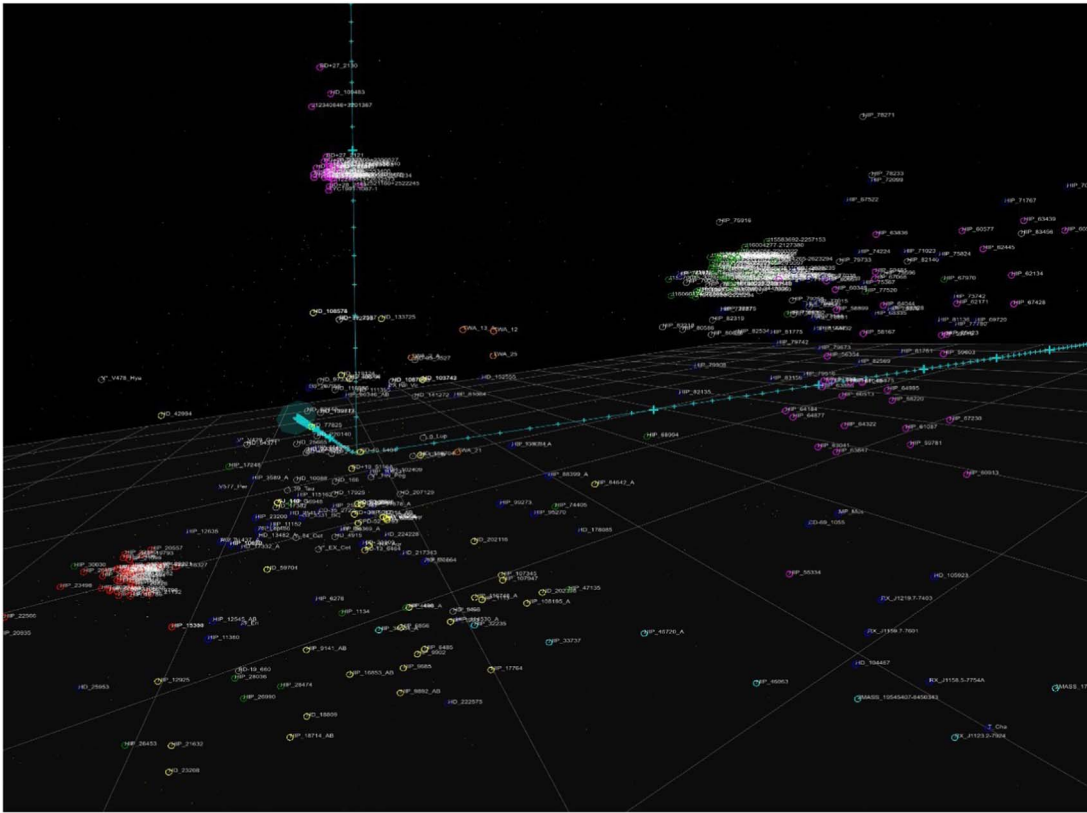


Figure 1. Screenshot of our PointCloudsVR simulation. This view would ordinarily be experienced through a virtual reality headset. Points represent the positions of stars in YSAs plotted in Galactic (X, Y, Z) coordinates. The app allows us to advance the positions of all the points forward (and move them backward) in time using Gaia DR2 velocities together with newly identified disk-hosting stars. Clearly visible are the Coma Ber (pink, top), Hyades (orange, lower left) Upper Scorpius (green, top right) associations, Octans (yellow). The X -axis points to the right, the Y -axis points to the left, and the Z -axis points up. The big tick marks on the X, Y, Z axes are 100 pc apart; the small ticks are 10 pc apart.

Doradus has been refined at 133^{+15}_{-20} Myr. It has also been suggested that the “stream” members do not all share a common age with the core members (Barenfeld et al. 2013). Note, however, that the Lee & Song (2019a) membership list does not appear to show this core + stream structure.

Our VR inspection revealed three new candidate disk-hosting members of this group to add to the list of possible AB Doradus members. Note that all of these stars have Gaia radial velocities (as do all the infrared-excess stars in this paper). All three of these stars lie on one side of the association, in the $-X, -Y$ direction (see the left panel of Figure 2). They were assigned low ($<7\%$) probabilities of membership in AB Doradus by BANYAN Σ , probably because of the dearth of known members at that XYZ position in the BANYAN Σ membership list. However, these new candidates have velocities resembling the average velocity of the known members (see Figure 2) and the presence of infrared excesses is a sign of youth.

HD 44775 (WISEA J062218.66-295134.7) is a proposed new AB Doradus member and an F3V at 105 pc. After we identified this proposed member in VR, we read that Oh et al. (2017) found this star to be part of a co-moving triple together with TYC 6518-1857-1 (98 pc) and CPD-25 1292 (96 pc). These two co-movers are shown as green arrows labeled T and C, respectively, in Figure 2.

HD 40540 (WISEA J055752.60-342834.1) is a proposed new AB Doradus member and an A8IV at 88 pc, and has a debris disk that was first recognized in IRAS data by Rhee et al. (2007). Later Spitzer spectroscopy revealed that the dust has a negligible crystallinity fraction ($<4\%$; Mittal et al. 2015).

HD 44510 (WISEA J061903.93-535823.9) is a proposed new AB Doradus member and an F3V at 108 pc. Cruz-Saenz de Miera et al. (2014) previously identified this star as having an infrared excess.

Figure 3 shows a color–magnitude diagram for AB Doradus, including the Gaia EDR3 field main sequence, shown in gray. The solid lines show isochrones at 10, 20, 30, ..., 100 Myr from Marigo et al. (2017) available online.¹⁶ The blue points show the previously identified members of AB Doradus from Lee & Song (2019a). The red and green x’s show our proposed new members: the red objects have infrared excess; the green are co-moving with them.

The members from Lee & Song (2019a) are barely distinguishable from the EDR3 field, consistent with the (Bell et al. 2015) age estimate of 149^{+51}_{-19} Myr, except perhaps at the reddest end of the CMD. Toward the blue end, where the new proposed members are, the isochrones are degenerate, making it even harder to constrain the ages of the new proposed members. This CMD highlights an important trend; the new members we discover using VR are often in a mass regime where isochrones are degenerate, making them hard to identify as group members in an isochronal analysis.

4.2. Argus

The Argus association (Torres et al. 2008) contains many stars within 100 pc of Earth, including the well-known debris

¹⁶ <http://stev.oapd.inaf.it/cmd>

Table 1
Candidate YSA Members with Disks Assigned Using VR

Gaia DR2 ID	Common Name/ WISE ID	Proposed YSA	Prev. Published Infrared Excess	Literature YSA	BANYAN Σ		W1–W4
					YSA	Prob	
2898071312314111488	HD 44775/ J062218.66-295134.7	AB Dor	1	None	ABDMG/ FIELD	0.8/99.2	0.517 ± 0.07
2889357751382351872	HD 40540/ J055752.60-342834.1	AB Dor	2, 3, 4, 5, 6, 7 9, 43	None	ABDMG/ FIELD	6.3/93.7	1.143 ± 0.07
5499867942228621056	HD 44510/ J061903.93-535823.9	AB Dor	8	None	ABDMG/ FIELD	1.9/98.1	0.533 ± 0.07
6470519830886970880	HD 198472/ J205241.67-531624.8	β Pic	5, 9, 10	β Pic (11 \dagger)	BPMG/ FIELD	70.6/29.4	0.519 ± 0.09
1336772153854267392	HD 157165/ J172007.53 + 354103.6	Oct Nr	14, 15	None	FIELD	99.9	0.439 ± 0.08
2517397846786452224	HD 15115/ J022616.32 + 061732.8	Tuc-Hor	3, 5, 9, 16, 17, 18 35, 36, 37, 38, 39, 40, 43, 44, 45, 47	β Pic (3, 19, 20, 29) AB Dor (21) Tuc-Hor (22, 40) Col (23)	THA/FIELD	98.6/1.4	0.545 ± 0.08
5247128354025136128	TYC 9196-2916-1/ J092521.90-673224.8	Tuc-Hor	No	None	LCC/FIELD	25.2/74.8	3.735 ± 0.04
2896173349085130112	HD 41992/ J060652.79-313054.1	Tuc-Hor	13	Col/Car (12)	THA/FIELD	1.4/98.6	0.836 ± 0.08
4881312593414911616	HD 30447/ J044649.55-261808.8	Col-Car	2, 3, 5, 9, 16, 17, 34, 41, 42, 43, 44, 46	Col (12, 19, 22, 24, 25)	COL/FIELD	99.5/0.5	0.872 ± 0.08
4867855155206070784	CPD-35 525/ J044115.76-351358.1	Col-Car	5	Col (26)	COL/FIELD	99.9/0.1	1.063 ± 0.09
5498909546046688256	CPD-57 937/ J060210.78-570142.1	Col-Car	5	None	COL/CAR FIELD	15.8/0.2/ 84.1	1.507 ± 0.07
2958833623399371392	HD 35841/ J052636.59-222923.8	Col-Car	3, 5, 27, 28 34, 41, 44, 46	Col (29, 30)	COL/FIELD	52.0/48.0	1.121 ± 0.08
4715896429133940352	HD 10472/ J014024.15-605956.7	Col-Car	2, 3, 4, 5, 9, 10, 16, 17, 43, 44, 46	Tuc-Hor (4, 20, 31, 32)	COL/FIELD	77.8/22.2	0.579 ± 0.08
4807752860334734720	HD 37852/ J053930.48-404102.4	Col-Car	9	Col (33 \dagger)	COL/FIELD	83.5/16.5	0.677 ± 0.07

References. (1) David & Hillenbrand (2015), (2) Rhee et al. (2007), (3) Chen et al. (2014), (4) Mittal et al. (2015), (5) Cotten & Song (2016), (6) Holland et al. (2017), (7) Kral et al. (2017), (8) Cruz-Saenz de Miera et al. (2014), (9) Wu et al. (2013), (10) Patel et al. (2014), (11) Crundall et al. (2019), (12) Gagné et al. (2021), (13) Silverberg et al. (2016), (14) Silverberg et al. (2018), (15) Kuchner et al. (2016), (16) Ballering et al. (2013), (17) Ballering et al. (2017), (18) Engler et al. (2019), (19) Malo et al. (2013), (20) Meshkat et al. (2017), (21) Gagné & Faherty (2018), (22) Vigan et al. (2017), (23) Bell et al. (2015), (24) Elliott et al. (2016), (25) Gagné et al. (2018b), (26) Gagné et al. (2018c), (27) Riviere-Marichalar et al. (2016), (28) Esposito et al. (2018), (29) Torres et al. (2008), (30) da Silva et al. (2009), (31) Torres et al. (2000), (32) Zuckerman et al. (2001b), (33) Faherty et al. (2018), (34) Moór et al. (2011), (35) Debes et al. (2008), (36) Rodigas et al. (2012), (37) Mazoyer et al. (2014), (38) Engler et al. (2019), (39) Lawson et al. (2020), (40) MacGregor et al. (2019), (41) Soummer et al. (2014), (42) Lazzoni et al. (2018), (43) Liu (2021), (44) Esposito et al. (2020), (45) Pawellek et al. (2021), (46) Moór et al. (2006), (47) Kalas et al. (2007). Kinematic match only have been marked with a \dagger .

Table 2
Co-movers and Companions to Candidate YSA Members with Disks Assigned Using VR

Gaia DR2 ID	Common Name/ WISE ID	Proposed YSA	Prev. Published Infrared Excess	Literature YSA	BANYAN Σ	
					YSA	Prob
2898402643271131264	TYC 6518-1857-1	AB Dor	No	1	ABDMG/FIELD	5.9/94.1
2911909593862390912	CPD-25 1292	AB Dor	No	1	ABDMG/FIELD	5.1/94.9
1336772325652957952	BD+35 2953	Oct Nr	2	3	N/A	N/A
4806146576925723264	HD 274311	Col-Car	4	1	COL/FIELD	52.8/47.2

References. (1) Oh et al. (2017), (2) Guillout et al. (2009), (3) Andrews et al. (2017), (4) Haakonsen & Rutledge (2009).

disk hosts β Leonis and 49 Ceti. Zuckerman (2019) argued for the physicality of this association and provided the most recent membership list and age estimate for this association: 40–50 Myr. We used this catalog of known Argus members, which includes nine stars with known infrared excesses. Our process recovered four previously identified members of Argus, including two disk-hosting stars previously identified by the Disk Detective project using the BANYAN Σ tool

(S. M. Silverberg et al. 2022, in preparation). However, our process did not recover any new candidate disk-hosting members of Argus.

4.3. β Pictoris

The well-studied β Pictoris (β Pic) moving group (Zuckerman et al. 2001a) appears to be one of the closest YSAs to the

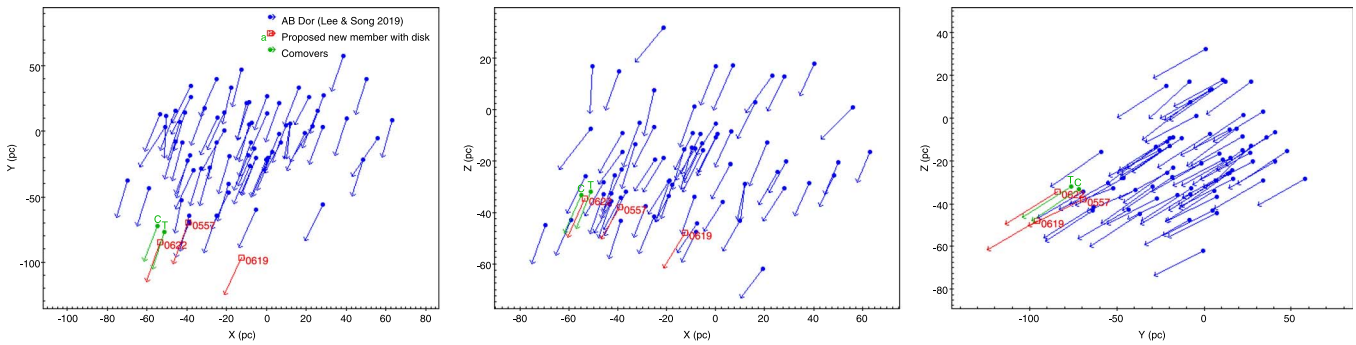


Figure 2. Previously identified members of AB Doradus from Lee & Song (2019a; blue), proposed new disk-hosting members of AB Doradus from Disk Detective (red) and co-moving stars (green), in XYZ (parsecs from the Sun) with vectors showing UVW (parsecs per 1000 yr). Of these candidates, J0622 is found in Table 5 of David & Hillenbrand (2015) as well as in co-moving catalogs Bochanski et al. (2018) and Oh et al. (2017) in a group of three co-moving stars (labeled in green as C and T). All three candidates were previously identified as infrared excess stars, but not as AB Doradus members.

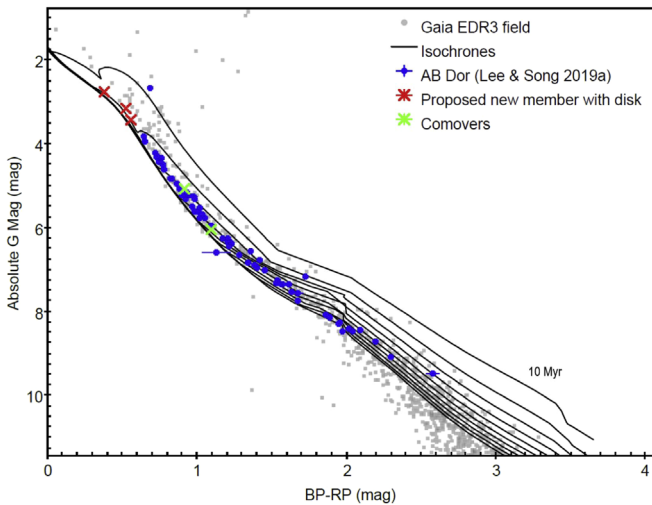


Figure 3. CMD of AB Doradus (blue) with proposed new members with disks (red) and co-movers (green) with isochrones from 10 Myr (top) to 100 Myr (bottom) and Gaia EDR3 field stars. The proposed new members lie in a sequence with the other AB Doradus members. Note how the isochrones tend to be degenerate toward the blue end of this diagram, where our proposed new disk-hosting members lie.

Sun, Miret-Roig et al. (2020) provide a useful overview of age estimates for this group. Miret-Roig et al. (2020) themselves present a dynamical trace-back age of $18.5^{+2.0}_{-2.4}$ Myr based on Gaia DR2. Recent estimates based on isochrone fitting (e.g., Mamajek & Bell 2014; Binks & Jeffries 2016) and estimates from lithium depletion boundary fitting (e.g., Binks & Jeffries 2014; Messina et al. 2016), perhaps the most reliable technique, hover around 24 Myr.

We first examined membership lists for β Pictoris from Gagné et al. (2018b, 2018c), Gagné & Faherty (2018) and Schneider et al. (2019), but then decided to use the more comprehensive membership list from Lee & Song (2019a), derived using machine learning and Gaia DR2.

We propose to assign HD 198472 to this group; this star was previously known to have an infrared excess (prior to Disk Detective). Our examination also suggests a new group assignment for HD 15115, one of the disk-hosting members listed in Lee & Song (2019a). Figure 4 depicts the group members from Lee & Song (2019a) in blue, and the two stars of interest (red and teal).

HD 198472 (WISEA J205241.67-531624.8) is a proposed β Pictoris member and an F 5/6 V star at a distance of 63 pc.

This star was first robustly identified as having an infrared excess by Wu et al. (2013). David & Hillenbrand (2015) found an isochronal age for this star of >1.5 Gyr. However, this star is kinematically identified with β Pictoris in Crundall et al. (2019), but this paper did not mention the infrared excess or any other signs of youth. Thus, the kinematics and the presence of an infrared excess suggest that an assignment of this star to β Pictoris should be considered seriously.

HD 15115 (WISEA J022616.32+061732.8) was identified as a member of β Pictoris by Lee & Song (2019a), but it has previously been associated with AB Doradus, Tuc-Hor, and Columba. The well-known edge-on debris disk around this star was discovered using the Hubble Space Telescope (HST) ACS High Resolution Channel (HRC) and confirmed with Keck adaptive optics using the near-infrared camera NIRC2 (Kalas et al. 2007). The debris disk has been resolved by the Hubble Space Telescope (HST) Near Infrared Camera and Multi-Object Spectrometer (NICMOS; Debes et al. 2008), Large Binocular Telescope (LBT; Rodigas et al. 2012), Gemini Near Infrared Coronagraphic Imager (NICI; Mazoyer et al. 2014), and Very Large Telescope (VLT) Spectro-Polarimetric High-contrast Exoplanet REsearch (SPHERE; Engler et al. 2019), and has also been spatially resolved by the Subaru Coronagraphic Extreme-AO and Coronagraphic High Angular Resolution Imaging Spectrograph (SCEXAO/CHARIS; Lawson et al. 2020). Atacama Large Millimeter Array (ALMA) imaging shows evidence for two rings in the disk separated by a cleared gap (MacGregor et al. 2019). The center and right panels of Figure 4 show that its velocity is a poor match for β Pictoris. We prefer to identify this infrared excess star with Tuc-Hor; further discussion about this star can be found below and in Figure 10 under Section 5.1.

We also recovered BD+45 598 (WISEA J022113.11+460006) which Hinkley et al. (2021) recently classified as a member of β Pictoris, and which Gagné et al. (2018b, 2018c), Gagné & Faherty (2018), Schneider et al. (2019), and Lee & Song (2019a) excluded from their membership lists. We found it to be a bit of an outlier based on its position, but a good match to β Pictoris based on its velocity. Overall, the quality of the match looks acceptable, so we support the conclusion of Moór et al. (2011) and Hinkley et al. (2021).

Figure 5 shows a CMD for β Pictoris, including the Gaia EDR3 field main sequence, shown in gray. The solid lines show isochrones at 10, 20, 30, 40, 50 Myr from Marigo et al. (2017) available online (see footnote 16). The blue points show the previously identified members of β Pictoris from

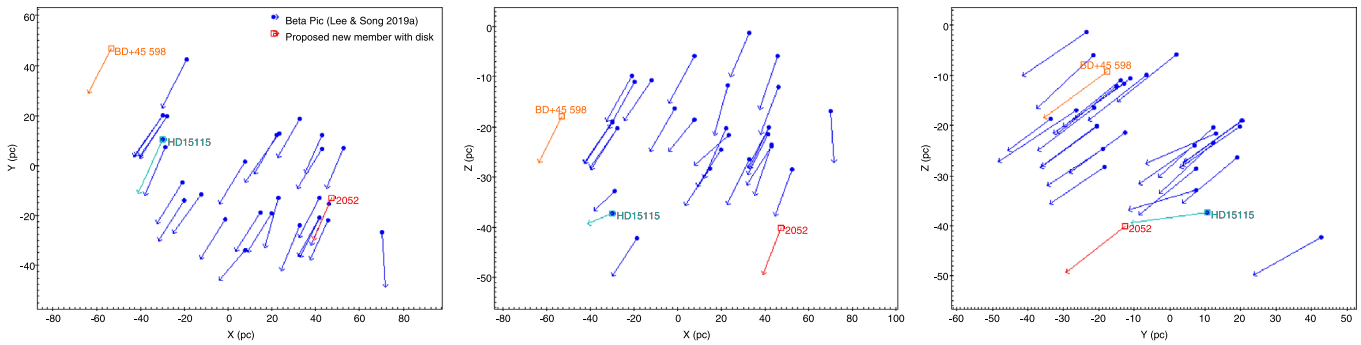


Figure 4. Previously identified members of β Pictoris (blue) from Lee & Song (2019a) and one new proposed disk-hosting group member (J205241.67-532624.8, shown in red) in XYZ (parsecs from the Sun) with vectors showing UVW (parsecs per 1000 yr). Our process also recovered BD+45 598 (J022113.11+460006) as a β Pic member (orange). The infrared excess star HD 15115 (J022616.32+061732.8; teal) was identified as a member of β Pic in the Lee & Song (2019a) catalog. However, its velocity stands out from the velocities of the other stars here, as you can see (especially in the right panel). We prefer to identify it with Tuc-Hor; further discussion about this star is found in Figure 10.

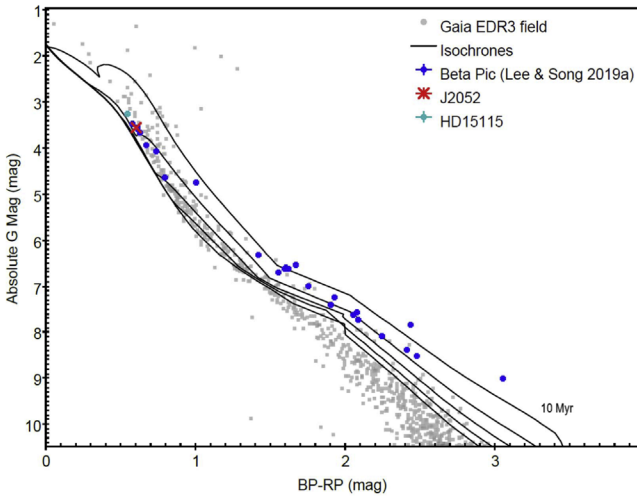


Figure 5. CMD of β Pictoris (blue) with proposed new member with disk J2052 (red) and HD 15115 (teal) with isochrones from 10 Myr (top) to 50 Myr (bottom) and Gaia EDR3 field stars.

Lee & Song (2019a). The red x shows our proposed new member that has infrared excess while the teal dot shows HD 15115.

The members from Lee & Song (2019a) are found above the main-sequence EDR3 field, consistent with Mamajek & Bell (2014), Binks & Jeffries (2016, 2014), and Messina et al. (2016) at around 24 Myr and our proposed new member appears to be consistent with the previously identified members of β Pictoris.

4.4. Octans-Near

Zuckerman et al. (2013) presented a list of 14 stars with UVW velocities resembling Octans, but located close to the Sun, called “Octans-Near” (Oct Nr; Figure 6). Mamajek (2016) asserted that this group “probably warrants stream status,” meaning that evidence for the coevolution of the Octans-Near stars was still thin. Indeed, the ages of the stars in this group range from 30 to 100 Myr according to Zuckerman et al. (2013). Both of these studies predate Gaia, however.

We applied our process to the Zuckerman et al. (2013) star list. We recovered one previously known member listed by Zuckerman et al. (2013): J034239.80-203243.3, which was discovered by Patel et al. (2014) to have an infrared excess. Additionally we identify two other stars that may be related to Octans-Near, which reside somewhat farther from the Sun than

the rest of Octans-Near, in the opposite direction from Octans. These, nonetheless, resemble Octans-Near in velocity and show signs of youth (infrared excess and X-ray emission). These stars are roughly 25 pc away from the edge of Octans-Near (in the Y direction); for comparison, Octans-Near spans about 40 pc in this direction.

HD 157165 (WISEA J172007.53+354103.6) This F8 star at 99 pc was one of the first 37 disk candidates published by the Disk Detective project (Kuchner et al. 2016). Follow-up imaging by the project using Palomar/Robo-AO searched for background objects in the Sloan-i filter within the 12'' radius of the WISE 4 Point-Spread Function and found none (Silverberg et al. 2018). Modeling of the spectral energy distribution of this system found the disk temperature of 196 ± 30 K and a fractional infrared excess of $L_{\text{IR}}/L_{\star} \approx 9.0 \pm 1.5 \times 10^{-5}$. This star has a wide companion, BD+35 2953, 89''/33 away, inferred by Andrews et al. (2017) from the Tycho-Gaia astrometric solution. See below.

BD+35 2953, another F8 star 99 pc distant from the Sun, is a wide companion to HD 157165. It is also the optical counterpart to a ROSAT All-Sky Survey X-ray source (Guillout et al. 2009). This star does not have a measured radial velocity in the Gaia DR2 catalog; therefore, the green arrow representing it in the figure shows only the proper motion components of its motion.

Figure 7 shows a CMD for Octans-Near, including the Gaia EDR3 field main sequence, shown in gray. The solid lines show isochrones at 10, 20, 30, 40, 50 Myr from Marigo et al. (2017) available online (see footnote 16). The blue points show the previously identified members of Octans-Near from Zuckerman et al. (2013). The red and green x’s show our proposed new members: the red object has infrared excess; the green is a wide companion co-moving with it.

The members from Zuckerman et al. (2013) are barely distinguishable from the EDR3 field, consistent with the age estimate of 30 to 100 Myr, with our proposed new member and co-mover consistent with the age as well.

4.5. TW Hya Association

Our process did not yield any new members of the TW Hya Association (Kastner 2016). We searched for new members of TW Hya, starting with a list of known members from Gagné et al. (2018b). There were no nearby Disk Detective stars so our choice of this list of known members did not matter much.

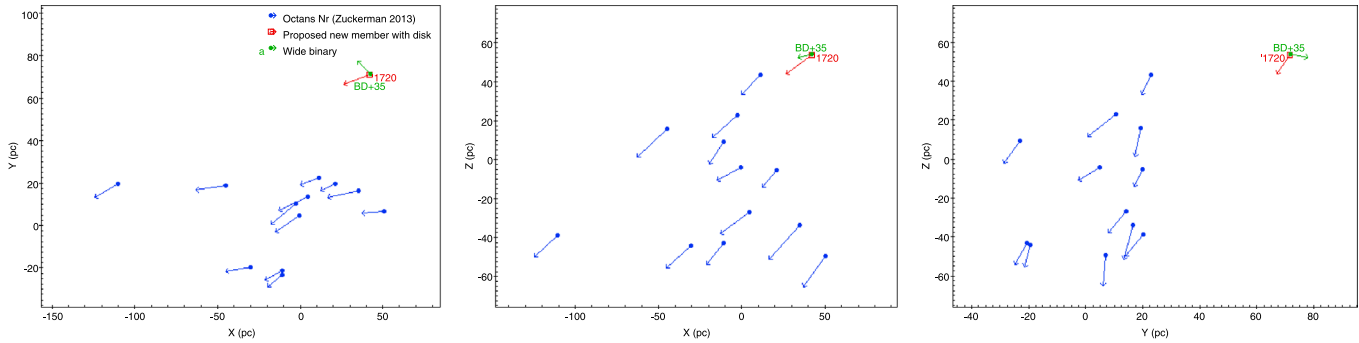


Figure 6. Members of Octans-Near (blue) previously proposed by Zuckerman et al. (2013), in XYZ (parsecs from the Sun) with vectors showing UVW (parsecs per 1000 yr). We identified two other stars that could be related to this group: the infrared excess star HD 157165 (J172007.53+354103.6), and a wide binary companion to this star (BD+35 2953) found by Andrews et al. (2017). Note that BD+35 2953 (wide binary) has no measured radial velocity so the length and direction of the green arrows are only based on two velocity components.

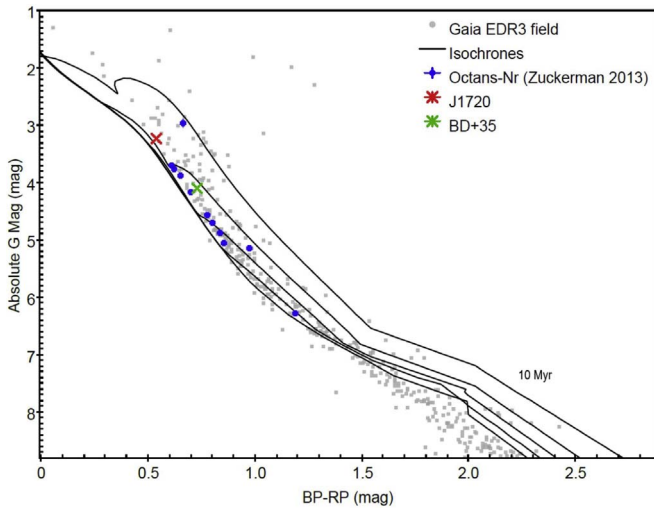


Figure 7. CMD of Octans-Near (blue) previously proposed by Zuckerman et al. (2013), with one proposed new member with disk J1720 (red) and wide binary companion (BD+35 2953) to this star (green) found by Andrews et al. (2017) with isochrones from 10 Myr (top) to 50 Myr (bottom) and Gaia EDR3 field stars.

5. Columba–Carina, Tucana–Horologium, and 32 Orionis

The Carina (Car), Columba (Col), and Tucana–Horologium (Tuc-Hor) groups overlap in position and velocity space. The 32 Orionis (32 Or) group lurks nearby these as well, at a similar velocity. Let us discuss these together.

Bell et al. (2015) determined the ages for three of these YSAs homogeneously through isochrone fitting: 45^{+11}_{-7} Myr for the Carina association, 42^{+6}_{-4} Myr for the Columba association, and 45 ± 4 Myr for the Tucana–Horologium moving group. In other words, the ages for these three groups are all consistent with one common age around 45 Myr. In contrast, Bell et al. (2017) estimates the age of 32 Or using isochronal fitting at 24 ± 4 Myr.

Recently, Lee & Song (2019a) proposed new membership lists for nine YSAs, including Carina, Columba, and Tuc-Hor. Then Lee & Song (2019b) reexamined the group assignments using two unsupervised machine-learning algorithms (K-means and Agglomerative Clustering), and argued for two new groups by recombining the memberships of 32 Or (ThOr), Columba, and Tuc-Hor. The discrepancies between these catalogs assembled by the same authors using different numerical tools

highlights the need for a new ab initio approach, and the need for the panoramic view afforded by our VR examination.

Figure 8 shows the positions and velocities for stars in these four groups. We suggest that, while 32 Or is similar in position space and motion as Columba, Carina, and Tuc-Hor, it is possible to distinguish it from these groups. The mean velocity of Tuc-Hor with the Smethells 165 group removed is $U = -9.944$, $V = -21.083$, $W = -0.524$. In comparison, the mean velocity of 32 Or is $U = -10.3390794$, $V = -19.54700395$, $W = -8.901980704$. Its velocity is greater in the $-W$ direction than that of the other groups, and it does not overlap in position space in the middle panel. We also did not find any new candidate members of 32 Or, so we will not discuss it further.

Rather, based on Figures 8 and 9, along with our VR examination, we have decided to first discuss Tuc-Hor, and then discuss Carina and Columba as one combined association, Columba–Carina.

Figure 9 shows the X , Y , Z , U , V , W positions and motion of the Lee & Song (2019a) catalog. Let us begin by ignoring the colors of the symbols, which may merely represent the history of how these YSAs were discovered. Now, consider all the objects to be part of a single large group. With this perspective, we see a reasonably tight cluster in velocity space; all but a handful of outliers lie within about 6 pc Myr^{-1} of one another. In position space, the stars are spread over about 100 pc in Z , and 150 pc in X and Y . The upper right panel and the lower middle panels show hints that the stars could be grouped into two separate clusters.

When we allow ourselves once again to consider the colors of the symbols, we see that the hint of a separation between two groups places Tuc-Hor entirely into one group, but cleaves Columba in two in position space. In the upper right panel about half of the Columba (blue) stars lie in the upper right next to the Tuc-Hor (turquoise) stars, while the other half are toward the middle of the panel.

Of the three proposed groups, Tuc-Hor seems perhaps the most distinct, at least in velocity (it overlaps with Columba in position). The Tuc-Hor stars (turquoise) are more tightly clustered in both position and velocity than either of the other groups, especially once we ignore the four stars that we have labeled as “Smethells 165 group” (magenta). Tuc-Hor stars clearly have the highest U , V , and W values (lower panels). The lower middle panel shows a possible slight gap between the Tuc-Hor stars and the others. They overlap somewhat with

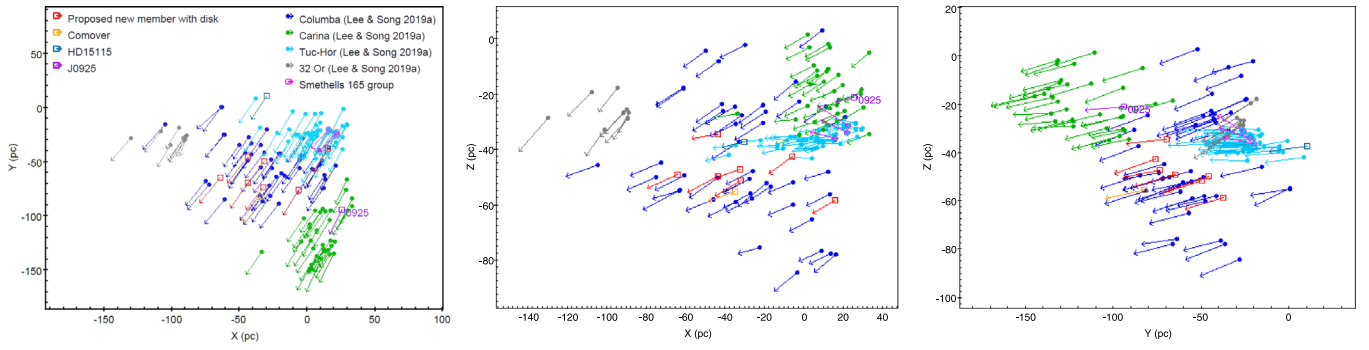


Figure 8. Proposed new members of Carina, Columba, and Tuc-Hor, together with known members according to Lee & Song (2019a) in XYZ (parsec from the Sun). The proposed new members of Columba–Carina and Tuc-Hor are the red squares, and the co-mover is the orange square. The extreme debris disk candidate, TYC 9196-2916-1 (J092521.90-673224.8), is the purple square. HD 15115 is the dark teal square. Columba are the filled blue dots, Carina are the filled green dots, Tuc-Hor are the filled turquoise dots, and 32 Or are the filled gray dots. The proposed Smethells 165 group members discussed in 5.2 are the magenta rings.

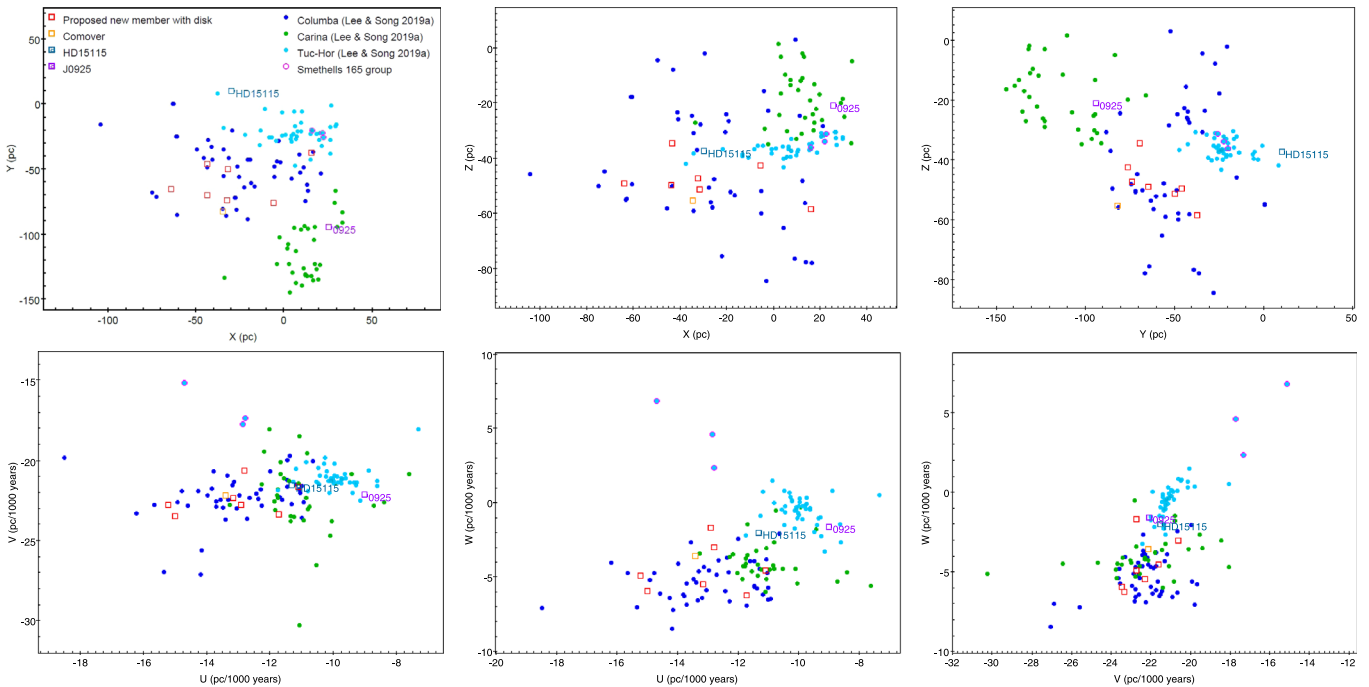


Figure 9. Proposed new members of Carina, Columba, and Tuc-Hor, together with known members according to Lee & Song (2019a) in XYZ (parsec from the Sun) in the top three frames and UVW (parsec per 1000 yr) in the bottom three frames. The proposed new members of Columba–Carina and Tuc-Hor are the red squares and the co-mover is the orange square. The extreme debris disk candidate, TYC 9196-2916-1 (J092521.90-673224.8), is the magenta square. HD 15115 is the dark teal square. Columba are the filled blue dots, Carina are the filled green dots, and Tuc-Hor are the filled turquoise dots. The proposed Smethells 165 group members are the magenta rings.

Columba stars in terms of position, but are relatively tightly constrained, occupying a range of only about 20 pc in Z.

5.1. Proposed Tucana–Horologium Association Members

Many authors have assembled catalogs of members of Tuc-Hor: Gagné et al. (2018b, 2018c), Gagné & Faherty (2018), and Schneider et al. (2019). Figure 10 shows the new inventory of Tuc-Hor by Lee & Song (2019a). Thanks to this work, the core members of this group are relatively well defined, and we do not have any new stars to add to the list of core members.

Our VR examination revealed two infrared excess stars that are within about 60 pc of Tuc-Hor (HD 41992 and TYC 9196-2916-1) and have space velocities very similar to that of the group. We propose that they could be perhaps former group members or members of an extended group corona. The Tuc-Hor association is elongated in the X direction and compact in

the Z direction; it is about 80 pc long in the X direction but only about 20 pc wide in Z. The two new loosely associated members we propose (HD 41992 and TYC 9196-2916-1) extend the group mostly in the Y direction.

Additionally, we advocate for the kinematic membership of the well-known disk host HD 15115 in Tuc-Hor; this membership has been a matter of debate (see below).

HD 41992 (WISEA J060652.79-313054.1) is an F8V at 89 pc, first identified as an infrared excess star by Disk Detective, as mentioned in Silverberg et al. (2016). Our VR inspection suggests relationships between this star and both Columba–Carina and Tuc-Hor; the star’s position places it closer to Columba–Carina, while its velocity resembles that of Tuc-Hor (Figure 10).

TYC 9196-2916-1 (WISEA J092521.90-673224.8) is a star of previously unknown spectral type at 100 pc, with no previous

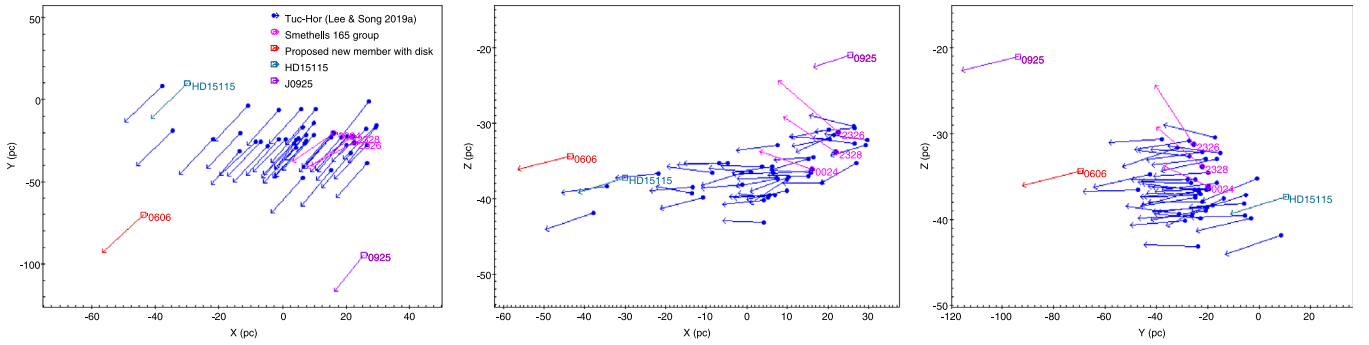


Figure 10. Previously identified members of Tucana–Horologium (blue) from Lee & Song (2019a) in XYZ (parsecs from the Sun) with vectors showing UVW (parsecs per 1000 yr). A newly identified loosely affiliated disk-hosting star (WISEA J060652.79-313054.1) is the red square, and another star, which is an extreme debris disk candidate (WISEA J092521.90-673224.8) is the purple square. Three stars that had been called bona fide members are shown in magenta. We propose that these three stars could be members of another group with an age similar to that of Tuc-Hor. We are calling this new group the “Smethells 165 group” after the brightest of the three stars. HD 15115 (J022616.32+061732.8), which hosts a well-known edge-on debris disk, is the dark teal square.

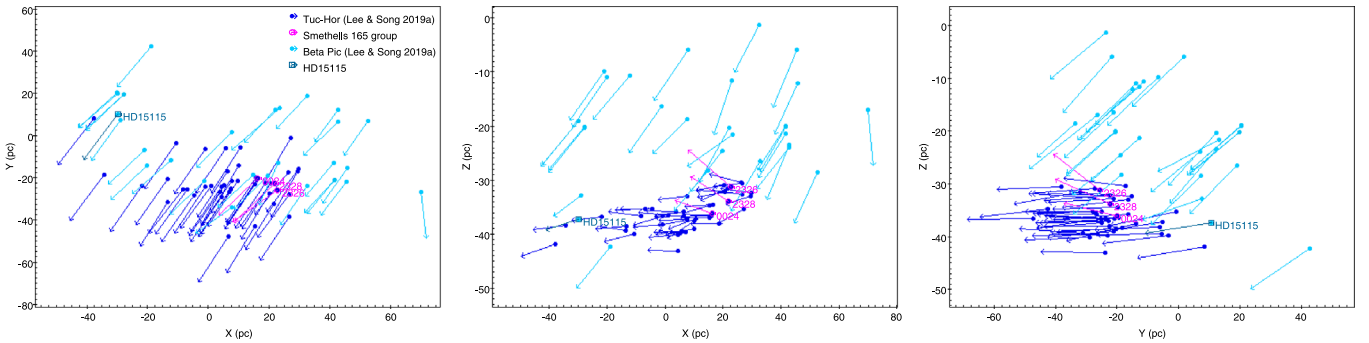


Figure 11. The well-known disk-hosting star HD 15115 (J022616.32+061732.8), shown as the dark teal square, was previously identified as a member of β Pictoris. However, its velocity and position are a better match for Tuc-Hor, as the middle and right panels of this figure reveal. Previously identified members of Tucana–Horologium (blue) and β Pictoris (turquoise) are from Lee & Song (2019a) in XYZ (parsecs from the Sun) with vectors showing UVW (parsecs per 1000 yr). The proposed Smethells 165 group is shown in magenta.

Table 3
Proposed Smethells 165 Group

2MASS Name	GAIA DR2 ID	Common Name	Spectral Type	U (pc per 1000 yr)	V (pc per 1000 yr)	W (pc per 1000 yr)
J00240899-6211042	4901926404913922816	Smethells 165	M0Ve (1)	−12.805	−17.350	2.391
J23261069-7323498	6380514358792367232	PM J23261-7323	M0Ve (1)	−14.706	−15.149	6.851
J23285763-6802338	6388014157668558080	UCAC4 110-129613	M2.5Ve (2)	−12.868	−17.728	4.638

References. (1) Torres et al. (2006), (2) Riedel et al. (2017a).

mentions in the literature. Disk Detective identified an apparent infrared excess from this star, which appears loosely associated with Tuc-Hor in our inspections. Our initial Markov Chain Monte Carlo (MCMC) fit to the photometry yielded a best-fit stellar temperature of 4400 K, implying a mid-K spectral type. It also revealed excess emission in all four WISE bands. Similar to HD 41992, our VR inspection suggests relationships between this star and both Columba–Carina and Tuc-Hor; the star’s position places it closer to Columba–Carina, while its velocity resembles that of Tuc-Hor (Figure 10). See Sections 6 and 7 for a more detailed discussion of this candidate “extreme debris disk” and its infrared excess.

HD 15115 (WISEA J022616.32+061732.8) F4 IV at 49 pc. Debes et al. (2008) estimated the star’s age to be 100–500 Myr, based on Ca ii H and K line indicators (Silverstone 2000), isochrone fitting (Nordström et al. 2004), and other indicators. Torres et al. (2008) proposed the star as a high-probability member of β Pictoris, and Malo et al. (2013) declared it a

member of the β Pictoris moving group (age 24 Myr). Later, Gagné et al. (2018b) examined it as a possible member of β Pictoris, but then rejected it as a bona fide member of that group based on a visual inspection. MacGregor et al. (2019) assigned it to Tuc-Hor based on BANYAN combined with Gaia coordinates and radial velocity. Our BANYAN-independent VR simulation supports this last assignment. Figure 11 shows the position and velocity of HD 15115 compared to the positions and velocities of β Pictoris and Tuc-Hor members from Lee & Song (2019a). The middle and right and middle panels show how HD 15115 is a better fit for Tuc-Hor.

5.2. A Group Containing Smethells 165

Our VR examination revealed that four previously identified Tuc-Hor members (2MASS J00240899-6211042, 2MASS J21551140-6153119, 2MASS J23261069-7323498, and 2MASS J23285763-6802338) from the Lee & Song (2019a) catalog match the group well in position space but do not match

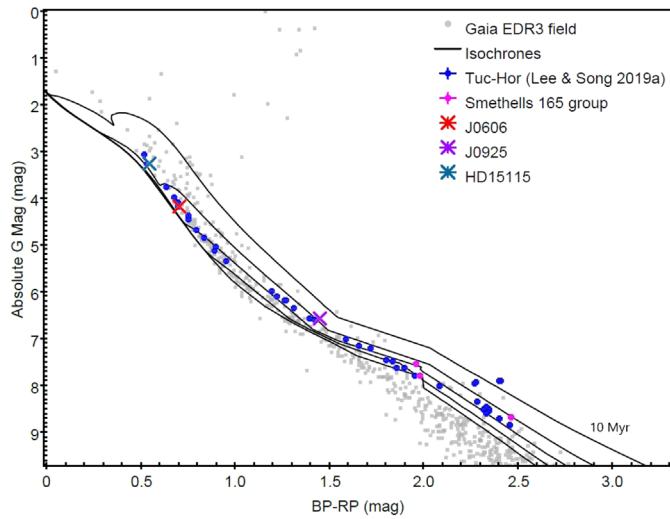


Figure 12. CMD of Tuc-Hor members, shown in blue. The proposed new member WISEA J060652.79-313054.1 is red, the proposed extreme debris disk candidate J0925 is purple, and HD 15115 (J022616.32+061732.8) is shown in dark teal. The proposed Smethells 165 group members are in magenta. Also shown are isochrones from 10 Myr (top) to 50 Myr (bottom) and Gaia EDR3 field stars in gray.

in velocity. One of these stars, 2MASS J21551140-6153119, does not have parallax in EDR3 so we set it aside. However, we suggest that the remaining three stars, listed in Table 3, and colored magenta in Figures 8, 9, 10, and 11, may not belong to Tuc-Hor after all. The mean velocity of these 3 stars in parsecs per 1000 yr is $U = -13.460$, $V = -16.742$, $W = 4.627$. Meanwhile, the mean velocity of the rest of Tuc-Hor is $U = -9.944$, $V = -21.083$, $W = -0.524$.

We looked to see if perhaps these three stars might be better matched to another nearby YSA like β Pictoris, Columba–Carina, or 32 Or. However, our visual inspection in VR suggests that they do not belong to any other YSA. They seem more likely to represent another new unknown group, perhaps with an age similar to Tuc-Hor, based on the CMD in Figure 12. We are calling this group the “Smethells 165 group”. Notably, these three stars are all M dwarfs (Torres et al. 2006; Riedel et al. 2017a).

5.3. Proposed Columba–Carina Members

Based on our VR examination, and analysis of Figures 8 and 9, we discuss Columba and Carina as one combined association, Columba–Carina. Our VR inspections suggest that Lee & Song (2019a) lists of Carina and Columba members need to be augmented with 6 additional members. These disk candidates are found in Table 1, and the co-mover can be found in Table 2. Figure 13 shows the positions and motions of these disk candidates compared to the Columba and Carina members listed by Lee & Song (2019a).

One star with an infrared excess that we propose as a new member of Columba–Carina has never been previously identified with a YSA: CPD-57 937. A second star with an infrared excess that we propose as a new member of Columba–Carina was previously proposed as a member of Tuc-Hor, but not of Columba or Carina: HD 10472. We also found four other stars with infrared excesses that we assign to Columba–Carina that were previously proposed as Columba–Carina members prior to Lee & Song (2019a): HD 30447, CPD-35 525, HD 35841, HD 10472, and HD 37852. This last star, HD 37852,

has an 83.5% likelihood of membership in Columba according to BANYAN Σ and a COL candidate in Faherty et al. (2018) and appears in S. M. Silverberg et al. (2022, in preparation). It has four co-movers according to Oh et al. (2017), which also likely belong to Columba–Carina.

CPD-57 937 (WISEA J060210.78-570142.1) This G5 star at 99 pc has not been previously proposed as a member of any YSA. Its infrared excess was previously noted by Cotten & Song (2016; on the “reserved” list, which consists of stars with IR excess from Tycho-2/ALLWISE without trigonometric parallaxes, and distance calculated using a spectral energy distributions (SED) fitting algorithm). Our inspection supports the assignment of this star to the combined Columba–Carina association.

HD 10472 (WISEA J014024.15-605956.7) This star has never been assigned to Columba–Carina, but it has been previously associated with Tuc-Hor Association by Mittal et al. (2015) and Meshkat et al. (2017). We find Columba–Carina to be a better match. Its infrared excess was previously noted by Cotten & Song (2016; on the “prime” list, which consist of stars within 120 pc of the Sun with IR excess from Tycho-2/ALLWISE). (Note that a footnote in Esposito et al. 2020 suggests that others may have been considering reassigning this object, but have not yet published their work.)

HD 35841 (WISEA J052636.59-222923.8) is an F3 V at 103.7 pc. Elliott et al. (2016) listed this object as a “candidate” member of Columba. Its infrared excess was previously noted by Cotten & Song (2016; on the “prime” list).

HD 30447 (WISEA J044649.55-261808.8): an F3 V at 81 pc. The debris disk around this star has been imaged by HST NICMOS (Soummer et al. 2014) and VLT SPHERE (Lazzoni et al. 2018). Gagné et al. (2018b, 2021) listed this star as a bona fide Columba member, as did Malo et al. (2013). BANYAN Σ gives a probability of membership in Columba of 99.5%. However, Lee & Song (2019a) did not list it as a member of this group. Our inspection supports the assignment of this star to the combined Columba–Carina association.

CPD-35 525 (WISEA J044115.76-351358.1) a G7 at 76 pc. This star was proposed as a candidate Columba member in Gagné et al. (2018c; and BANYAN Σ gives a probability of membership in Columba of 99.9%), but it is not included as a member by Lee & Song (2019a). Its infrared excess was previously noted by Cotten & Song (2016; on their “prime” list). Our inspection supports the assignment of this star to the combined Columba–Carina association.

HD 37852 (WISEA J053930.48-404102.4) is a B8V at 93 pc. BANYAN Σ provides a probability of membership in Columba of 83.5% for this star, so we discuss it further in S. M. Silverberg et al. (2022, in preparation). This star’s WISE excess was first identified by Wu et al. (2013). Oh et al. (2017) found HD 37852 to be co-moving with four other stars, three of which were included in Lee & Song (2019a) as members of Columba. The fourth of these co-movers is HD 274311.

HD 274311 is a K5e at 105 pc. This star is listed as a ROSAT bright source by Haakonsen & Rutledge (2009). This is part of Group 55 in Oh et al. (2017), which has only five members.

Figure 14 shows a CMD for Carina, Columba and Tuc-Hor, including the Gaia EDR3 field main sequence, shown in gray. The solid lines show isochrones at 10, 20, 30, 40, 50 Myr from Marigo et al. (2017) available online (see footnote 16). The blue dots show the previously identified members of Columba,

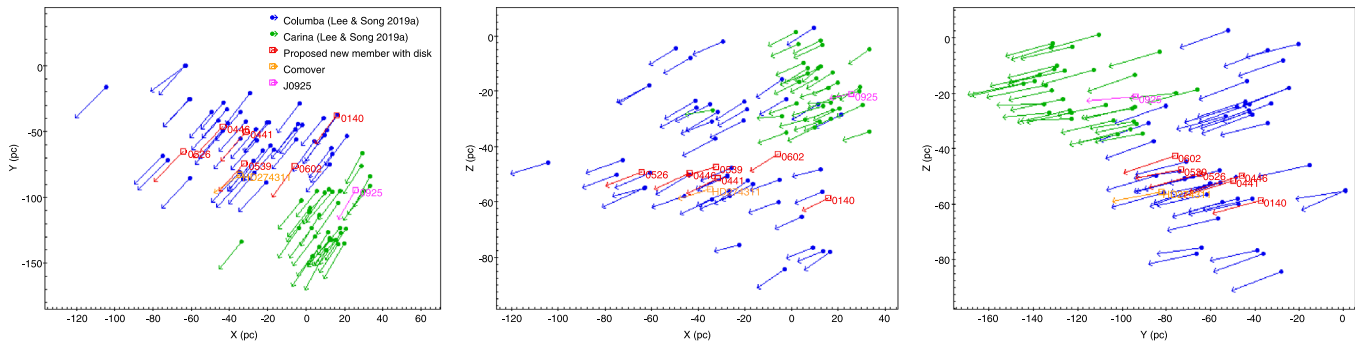


Figure 13. Proposed new disk-hosting kinematic members of Columba–Carina (red), with co-mover (orange), extreme debris disk candidate J0925 (magenta), and previously identified members of Columba (blue) and Carina (green) from Lee & Song (2019a) in XYZ (parsecs from the Sun) with vectors showing UVW (parsecs per 1000 yr).

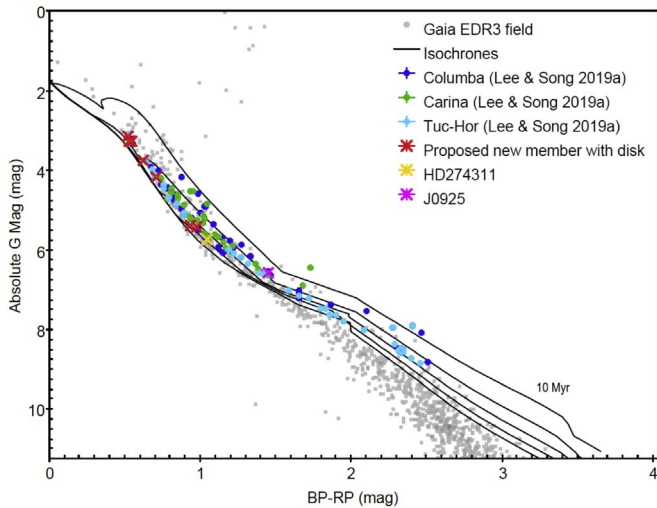


Figure 14. CMD of Carina (green), Columba (blue) and Tuc-Hor (turquoise) with proposed new members with disks (red), co-mover HD 274311 (orange) and proposed extreme debris disk candidate J0925 (magenta) with isochrones from 10 Myr (top) to 50 Myr (bottom) and Gaia EDR3 field stars. New association members we discover using VR are often in a mass regime where isochrones are degenerate.

the green dots show Carina, and the turquoise dots show Tuc-Hor, all from Lee & Song (2019a). The red x’s show our proposed new members: the red objects have infrared excess, the orange x is co-moving with them, and the magenta x shows the proposed extreme debris disk.

Toward the reddest end, the members from Lee & Song (2019a) are found above the EDR3 field, consistent with the Bell et al. (2015) common age estimate of around 45 Myr. In general, the proposed new members are consistent with the previously identified members. However, toward the blue end, where some new proposed members are, the isochrones are degenerate, making it even harder to constrain the ages of the new proposed members. Once again, this CMD highlights the trend that new members we discover using VR are often in a mass regime where isochrones are degenerate, making them hard to identify as group members in an isochronal analysis.

6. Discussion: Spectral Energy Distributions

Most of the infrared excess stars we identified as new YSA members only have significant excess emission in the W4 band. The W1–W4 colors of all the stars are listed in Table 1. However two of the newly identified YSA members show

evidence for excess emission in multiple bands: J044115.76-351358.1 and J092521.90-673224.8. We modeled the SEDs for these two systems to help us better understand the distribution of circumstellar material in them (Figure 15).

As an initial step in the modeling process, we iteratively fit a BT-Settl/CIFIST model (Baraffe et al. 2015) to the observed photometry using maximum likelihood estimation (MLE). We initially fit only the three Gaia DR2 photometry points and the 2MASS J point. Then we checked to see if the photometry in the next band (the shortest wavelength not included in the fit) was in excess (more than 5σ above the flux predicted by the stellar model). If that next longer band did not show an excess, we redid the fit now including the photometry from this next longer wavelength band. We continued this process, adding new bands to the fit, until we either identified a photometric excess or all bands except W3 and W4 were included in the fit. This iterative method ensures that we did not accidentally incorporate points in our fit for the photosphere that contain excess emission. This model for the stellar photosphere yields T_{eff} , $\log(g)$, and r_*/d , the ratio of stellar radius to distance.

Using these parameters derived from this model for the stellar photosphere, we then modeled the excess emission using one or two blackbody functions, corresponding to one or two single-temperature dust belts. We fit these to the excess emission using MLE as well, finding for each dust belt the temperature T_{disk} and x_{disk} , a parameter that includes the number density of dust grains, the dust grain radius, and the optical depth of the dust. Once these dust parameters were derived, we then re-fit the entire system to find the optimum values of the continuous variables (r_{star}/d , T_{disk} , x_{disk} , and in the case of a two-disk fit $T_{\text{disk},2}$, $x_{\text{disk},2}$) using maximum likelihood estimation, keeping our best-fit T_{eff} and $\log(g)$ constant. We adopted the parameters derived from this new fit as our final values for the system. To estimate the uncertainties on these variables, we then ran a 5000-step MCMC routine using emcee (Foreman-Mackey et al. 2013). This process yields the 5th and 95th percentile values for each of the variables.

For the first system, J044115.76-351358.1, the star is best fit as a 5500 K G-type star, and the infrared excess is well fit with a single-temperature blackbody. The excess has a best-fit temperature of 253^{+39}_{-23} K, and best-fit L_{IR}/L_{\star} of $6.27^{+0.69}_{-0.74} \times 10^{-4}$. These values are typical for warm debris disks.

The second star, TYC 9196-2916-1 (J092521.90-673224.8), merits a longer discussion. As Figure 15 shows, the infrared excess has multiple components. Additionally, the best-fit

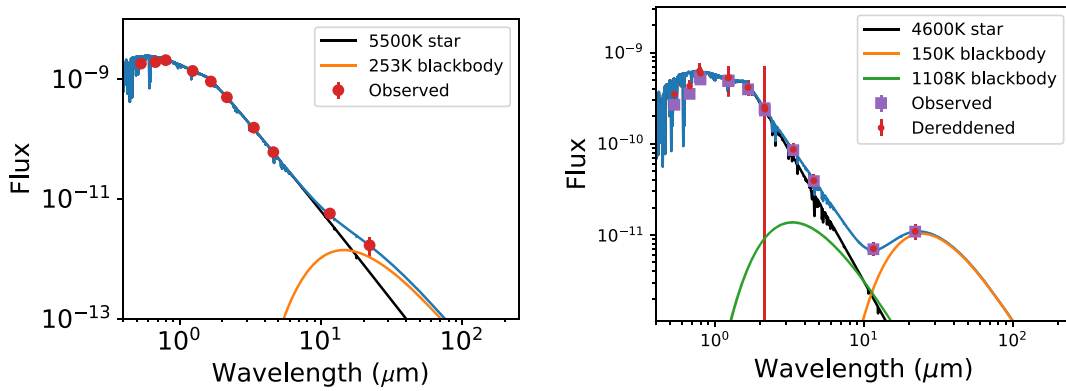


Figure 15. SEDs for J0441 (left) and J0925 (right). The photometry comes from Gaia DR2, 2MASS, WISE, and (for J0925) the Deep Near Infrared Survey of the Southern Sky (DENIS). Each star is fit by a BT-Settl/CIFIST stellar model (Baraffe et al. 2015), and the infrared excess is modeled by one or two blackbody functions. Data for J0925 are dereddened following the Fitzpatrick (1999) dereddening law as modified by Indebetouw et al. (2005). Note that the hot component of the excess emission from J0925 is variable, according to WISE photometry.

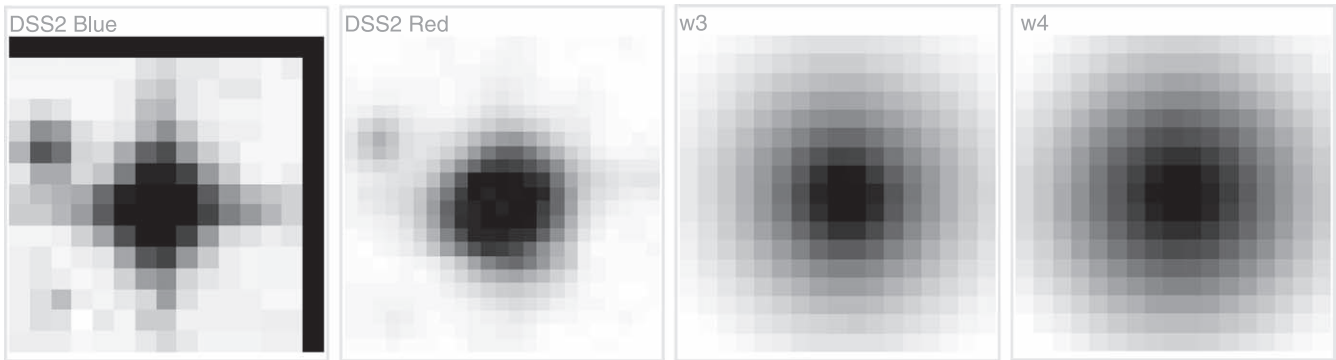


Figure 16. Images of J092521.90-673224.8 in DSS blue, DSS red, WISE 3, and WISE 4. Each postage stamp is $24'' \times 24''$ in angular extent. The background objects visible on the left of the DSS images do not seem to appear in the WISE images, implying that they do not explain the large excess emission measured in the W3 and W4 bands.

temperature and $\log(g)$ from our initial process ($T_{\text{eff}} = 4400$ K, $\log(g) = 3.5$) significantly disagree with the spectroscopically derived values for the star ($T_{\text{eff}} = 4607 \pm 85$ K, $\log(g) = 4.49 \pm 0.18$) from the third data release from the Galactic Archaeology with Hermes project (GALAH DR3; Buder et al. 2021), suggesting that interstellar extinction plays a significant role for this source. To account for this extinction, we used the Virtual Observatory SED Analyzer (VOSA; Bayo et al. 2008), which incorporates extinction, to fit all available photometry at a wavelength shorter than $1 \mu\text{m}$, avoiding photometry that could be significantly impacted by the observed excess. We again used BT-Settl/CIFIST models, using only those models within 100 K of the T_{eff} and 1 dex of the $\log(g)$ for the source found in GALAH DR3, to obtain a best-fit stellar model and extinction. We then used this best-fit model and extinction, and fit the excess with blackbody functions as described above.

We found that the best-fit model for this source was an SED with a two-component blackbody excess, with temperatures 150^{+37}_{-13} K and 1108^{+278}_{-393} K and a total $L_{\text{IR, warm}}/L_{\star} \approx 1.6 \times 10^{-2}$ and $L_{\text{IR, hot}}/L_{\star} \approx 2.1 \times 10^{-2}$. Using Equation (3) from Backman & Paresce (1993) and our best-fit temperatures and stellar luminosity ($L_{\star} \approx 0.267L_{\odot}$), the blackbody radius of the outer disk for J0925 is ~ 1.77 au, while the blackbody radius for the inner disk is ~ 0.03 au. We also derive a surface area for the warm disk of ~ 0.63 au², and for the hot disk of $\sim 3 \times 10^{-4}$ au². Assuming 10-micron silicate grains, the dust mass of

the warm disk is $\sim 8 \times 10^{-3}$ lunar masses, while the dust mass of the hot disk is $\sim 3 \times 10^{-6}$ lunar masses. This ignores larger bodies (e.g., comets) that could contain the bulk of the mass.

7. J0925: An Extreme Debris Disk

The Disk Detective citizen science project originally classified TYC 9196-2916-1 (J092521.90-673224.8) as a “multiple,” probably because of the DSS Blue, Red, and IR images, which show two background sources, roughly $8''$ away. Disk Detective was constructed to search for stars with reliable excess at W4, and objects at this separation would be potential sources of confusion in the W4 band. However, this object has a strong excess at W3 and W4 (Figure 16), and those background sources are not visible at all in either 2MASS or WISE images, so they could not be contributing at all to the excess at W3, and probably do not substantially contribute to the W4 excess either.

We triple checked the images of this star (also known as subject AWI00063mu in the Disk Detective v1 catalog) for contamination using the IRSA finder chart, and found none. This star is too far south to have images in the Pan-STARRS archive. The nearest star in Gaia EDR3 is $11''$; for comparison, WISE channels 1, 2, and 3 all have point-spread functions with an FWHM of about $6''$, while WISE channel 4 has a FWHM of about $12''$. The star was classified by citizen scientists Jonathan Holden and Phillip Griffith Sr.

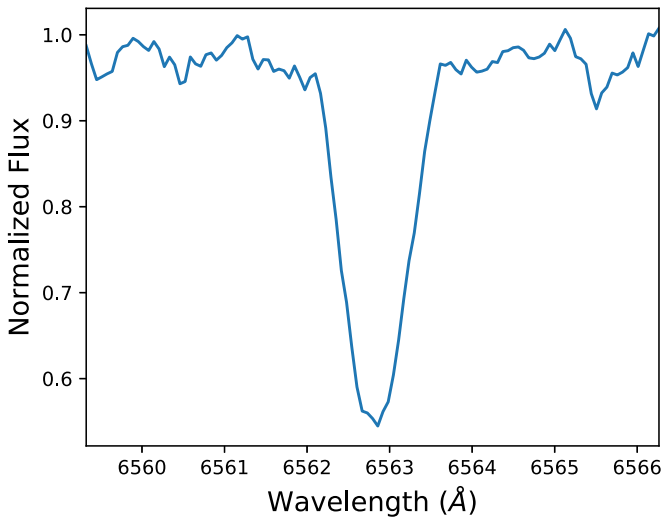


Figure 17. The spectrum of the $H\alpha$ line for J0925 from GALAH exhibits clear absorption, indicating no ongoing accretion.

Intriguingly, this star is reported as an emission line star by Čotar et al. (2021) based on a spectrum from the GALAH survey. This paper initially led us to speculate that J0925 could be hosting a Peter Pan disk, even though it is a K-type star. Other known Peter Pan disk hosts are primarily M stars, which may be a consequences of disk dispersal physics (Wilhelm & Portegies Zwart 2022). However, an inspection of the GALAH spectrum (Figure 17) shows $H\alpha$ to clearly be in absorption rather than emission, indicating that there is likely no ongoing accretion.

Curiously, the AllWISE variability flags for J092521.90-673224.8 indicate that this source is variable in W1, W2, and W3. This variability is similar to that seen for the hot-temperature component of the Peter Pan disk W0808 (Murphy et al. 2018), in that it appears correlated in the W1 and W2 bands (with limited time-series data available at W3 compared with the data available at W1 and W2 from the Near Earth Object Wide-field Infrared Survey Explorer (NEOWISE)-R), with variations ~ 0.392 mags in both W1 and W2. However, such variability is also thought to be an inherent characteristic of extreme debris disks (Meng et al. 2012; Su et al. 2019; Moór et al. 2021). Indeed, looking at the WISE data in terms of “excess fraction” (i.e., the stellar-photosphere-subtracted flux as a fraction of the flux from the photosphere) shows variations of $\sim 40\%$ at W1 and $\sim 50\%$ of the underlying flux at W2. By comparison, Su et al. (2019) found variations of $\sim 20\%$ at $3.6 \mu\text{m}$ and $\sim 60\%$ at $4.5 \mu\text{m}$ for the ID8 system, which correspond to the lower temperature of the “hot” excess in that system compared to J0925. This indicates that J0925 can quite reasonably be explained as an extreme debris disk.

Balog et al. (2009), Meng et al. (2015), and Moór et al. (2021) describe extreme debris disks (EDDs) as warm disk-hosting stars between 10 and 200 Myr in age, with unusually high fractional luminosities and strong mid-IR excess emission. The dust temperature of these EDDs are found to be >300 K, and the fractional luminosity >0.01 is about three orders of magnitude higher than normally found in debris disks (Balog et al. 2009; Moór et al. 2021). The high dust luminosity could be due to recent collision events and their aftermath Schneider et al. (2013). Relatively few EDDs are known; Moór et al. 2021 lists a sample of “all known EDDs” containing only 17 stars.

We are not aware of any other K-type extreme debris disks in Columba–Carina. However, the F5V Columba member HD 35841 hosts a debris disk with a fractional infrared excess of $L_{\text{IR}}/L_{\star} \approx 10^{-3}$. Much of this excess arises from a narrow circular ring at $r = 19\text{--}20$ au, based on images from HST and Gemini (Esposito et al. 2018). For comparison, J0925 appears to have more dust with an $L_{\text{IR}}/L_{\star} \approx 16$ times that of HD 35841.

Other young stellar associations do have K-type stars with extreme debris disks. Zuckerman (2015) discovered V488 Per, a K-type star with an age of 90 Myr. With a characteristic temperature of ~ 800 K, this dust orbits only ~ 0.06 au from the star (assuming blackbody grains). This star appears to have more dust with a L_{IR}/L_{\star} of ~ 0.16 which is ≈ 10 times that of J0925.

Another interesting K star with an extreme debris disk is TYC 8241-2652-1, a K2V in LCC (Goldman et al. 2018). Curiously, the mid-IR luminosity of this star was observed to decay significantly over less than two years. It began with a warm (~ 450 K), unusually dust-rich disk with a $L_{\text{IR}}/L_{\star} \approx 0.11$, and evolved into a colder (<200 K), more tenuous disk with a $L_{\text{IR}}/L_{\star} \sim 10^{-3}$ (Melis et al. 2012). Pecaú & Mamajek (2016) found this star to have a spectral type of K3IV(e) and assigned it to the Scorpius–Centaurus OB association, with an age of 14 Myr. For comparison, J0925 appears to be in between the two extremes of this star in terms of luminosity of its disk.

8. Theia Groups

The moving groups discussed above are clustered in position, velocity and age. But Kounkel & Covey (2019) drew attention to the notion of diffuse moving groups, clustered in velocity and age but relatively unclustered in position. Kounkel & Covey (2019) used unsupervised machine learning on Gaia DR2 data to find 1901 such diffuse groups of co-moving stars, calling them “Theia” groups.

Subsequently, (Gagné et al. 2021, GFMP21) proposed that 14 of these Theia groups may be kinematically related to the YSAs discussed in Sections 4 and 5. This observation led GFMP21 to suggest that some of these moving groups are possibly tidal tails from more distant open clusters. In the process, GFMP21 found that several of the disk candidates and co-moving stars listed in Tables 1 and 2 could be associated with Theia groups: Theia 92, Theia 208, and Theia 301. Here is a summary of these assignments suggested by GFMP21.

HD 41992/WISEA J060652.79-313054.1—GFMP21 assigned this object to Theia 208, which they argued is likely related to Columba and Carina. We found that this star has a position consistent with membership in Columba–Carina, but a velocity consistent with membership in Tuc-Hor, as shown in Figure 10.

HD 35841/WISEA J052636.59-222923.8—GFMP21 assigned this star to Theia 208.

HD 274311/Gaia DR2 4806146576925723264—GFMP21 found this object to be part of Group 55 in Oh et al. (2017), which has only five members. Group 55 is near Theia 208, but not part of it.

HD 44775/WISEA J062218.66-295134.7—GFMP21 assigned this star to Theia 301; Kounkel & Covey (2019) and GFMP21 suggested that Theia 301 might be related to AB Doradus.

HD 40540/WISEA J055752.60-342834.1—same as above.

HD 44510/WISEA J061903.93-535823.9—same as above.

TYC 6518-1857-1/Gaia DR2 2898402643271131264—same as above.

CPD-25 1292/Gaia DR2 2911909593862390912—same as above.

9. Conclusions

We examined eight nearby young moving groups using a novel VR technique and found seven new likely disk-hosting members of these groups. Each one of these stars is likely to be a valuable target for coronagraphic imaging. The infrared excesses for most of our objects of interest had been previously identified in other searches, except for two stars, which Disk Detective first identified as having infrared excess (J092521.90-673224.8 and J060652.79-313054.1). We also identified four other likely new members of these moving groups that do not have disks, but which are co-movers with other new members. We suggested that three M dwarfs, previously considered members of Tuc-Hor are better considered a separate moving group, tentatively called Smethells 165.

These findings demonstrate the value of new visual examinations of the shapes and memberships of these moving groups, and VR as a tool for performing such examinations. Note that none of these objects was identified by BANYAN Σ as a high-probability group member (we are saving a discussion of group members identified via BANYAN Σ for a future paper). Furthermore, our VR technique identified new candidate members often found in a mass regime where isochrones are degenerate, which highlights the unique value that the VR tool demonstrates in this area.

The new proposed group members include two stars (J092521.90-673224.8 and HD 41992) with positions consistent with membership in Columba–Carina, but velocities consistent with membership in Tuc-Hor. They may have been neglected by earlier studies for exactly this reason. One of these, *TYC 9196-2916-1 (J092521.90-673224.8)*, appears to host an extreme debris disk with a two-component infrared excess of $L_{\text{IR,warm}}/L_{\star} \approx 1.6 \times 10^{-2}$ and $L_{\text{IR,hot}}/L_{\star} \approx 2.1 \times 10^{-2}$. Its characteristics are not unusual when compared to other K-type extreme debris disks.

Since we completed this work, Gaia Early Data Release 3 (EDR3) has come out, and a new version of the Disk Detective citizen science project has launched. Disk Detective 2.0 utilizes the Zooniverse Panoptes platform and targets a Gaia-selected sample of nearby systems as opposed to a photometrically selected sample. This updated project has the express goals of finding new YSA members and new Peter Pan disks. We expect VR to help us with this second generation project as well.

The authors thank Sarah Logsdon, Michaela Allen, Petr Pokorný, and Veselin Kostov for helpful discussions, and Joel Kastner for valuable advice and expertise. SH thanks Professor Hugh Hill at International Space University (ISU) for unwavering encouragement and support.

The authors acknowledge support from grant 14-ADAP14-0161 from the NASA Astrophysics Data Analysis Program and grant 16-XRP16_2-0127 from the NASA Exoplanets Research Program. M.J.K. acknowledges funding from the NASA Astrobiology Program via the Goddard Center for Astrobiology. Support for this work was provided by NASA through the Space Telescope Science Institute’s Directors Discretionary

Research Fund (DDRF). The Space Telescope Science Institute is operated by AURA, Inc., under NASA contract NAS 5-26555. The material is based upon work supported by NASA under award number 80GSFC21M0002.

This publication makes use of data products from the Wide-Field Infrared Survey Explorer, which is a joint project of the University of California, Los Angeles, and the Jet Propulsion Laboratory (JPL)/California Institute of Technology (Caltech), and NEOWISE, which is a project of JPL/Caltech. WISE and NEOWISE are funded by NASA.

This work has made use of data from the 2MASS project and the Digitized Sky Survey. 2MASS is a joint project of the University of Massachusetts and the Infrared Processing and Analysis Center (IPAC) at Caltech, funded by NASA and the NSF. The Digitized Sky Survey was produced at the Space Telescope Science Institute under U.S. Government grant NAG W-2166. The images of these surveys are based on photographic data obtained using the Oschin Schmidt Telescope on Palomar Mountain and the UK Schmidt Telescope. The plates were processed into the present compressed digital form with the permission of these institutions.












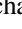


This work has made use of data from the European Space Agency (ESA) mission Gaia (<https://www.cosmos.esa.int/gaia>), processed by the Gaia Data Processing and Analysis Consortium (DPAC, <https://www.cosmos.esa.int/web/gaia/dpac/consortium>). Funding for the DPAC has been provided by national institutions, in particular the institutions participating in the Gaia Multilateral Agreement.

This research has made use of the SIMBAD database, operated at CDS, Strasbourg, France. Some of the data presented in this paper were obtained from the Mikulski Archive for Space Telescopes (MAST). STScI is operated by the Association of Universities for Research in Astronomy, Inc., under NASA contract NAS5-26555. Support for MAST for non-HST data is provided by the NASA Office of Space Science via grant NNX13AC07G and by other grants and offices. This research has made use of the VizieR catalog access tool, CDS, Strasbourg, France (DOI : [10.26093/cds/vizier](https://doi.org/10.26093/cds/vizier)). The original description of the VizieR service was published in Ochsenein et al. (2000).

This research has also made use of the Tool for Operations on Catalogues And Tables (TOPCAT) graphical application (<http://www.starlink.ac.uk/topcat/>, Taylor 2005).


Facilities: CTIO:2MASS, Sloan, WISE, Gaia.

ORCID iDs

Susan Higashio  <https://orcid.org/0000-0002-9470-7802>
 Marc J. Kuchner  <https://orcid.org/0000-0002-2387-5489>
 Steven M. Silverberg  <https://orcid.org/0000-0002-3741-4181>
 Jonathan Gagné  <https://orcid.org/0000-0002-2592-9612>
 John H. Debes  <https://orcid.org/0000-0002-1783-8817>
 Joshua Schlieder  <https://orcid.org/0000-0001-5347-7062>
 John P. Wisniewski  <https://orcid.org/0000-0001-9209-1808>
 Stewart Slocum  <https://orcid.org/0000-0003-1740-3407>
 Alissa S. Bans  <https://orcid.org/0000-0003-0426-7987>
 Shambo Bhattacharjee  <https://orcid.org/0000-0002-0862-9108>
 Joseph R. Biggs  <https://orcid.org/0000-0002-2405-6856>
 Milton K. D. Bosch  <https://orcid.org/0000-0002-9766-2400>
 Tadeas Cernohous  <https://orcid.org/0000-0002-9622-9605>
 Katharina Doll  <https://orcid.org/0000-0002-2993-9869>

Hugo A. Durantini Luca  <https://orcid.org/0000-0002-4143-2550>

Alexandru Enachioaie  <https://orcid.org/0000-0002-4020-8100>

Jonathan Holden  <https://orcid.org/0000-0002-1104-4442>

Michiharu Hyogo  <https://orcid.org/0000-0001-8343-0820>

Lisa Stiller  <https://orcid.org/0000-0002-1825-7133>

References

- Andrews, J. J., Chanamé, J., & Agüeros, M. A. 2017, *MNRAS*, **472**, 675
- Backman, D. E., & Paresce, F. 1993, in *Protostars and Planets III*, ed. E. H. Levy & J. I. Lunine (Tucson, AZ: Univ. Arizona Press), 77
- Ballerling, N. P., Rieke, G. H., Su, K. Y. L., & Gáspár, A. 2017, *ApJ*, **845**, 120
- Ballerling, N. P., Rieke, G. H., Su, K. Y. L., & Montiel, E. 2013, *ApJ*, **775**, 55
- Balog, Z., Kiss, L. L., Vinkó, J., et al. 2009, *ApJ*, **698**, 1989
- Baraffe, I., Homeier, D., Allard, F., & Chabrier, G. 2015, *AA*, **577**, A42
- Barenfeld, S. A., Bubar, E. J., Mamajek, E. E., & Young, P. A. 2013, *ApJ*, **766**, 6
- Bayo, A., Rodrigo, C., Barrado Y Navascués, D., et al. 2008, *A&A*, **492**, 277
- Bell, C. P. M., Mamajek, E. E., & Naylor, T. 2015, *MNRAS*, **454**, 593
- Bell, C. P. M., Murphy, S. J., & Mamajek, E. E. 2017, *MNRAS*, **468**, 1198
- Binks, A. S., & Jeffries, R. D. 2014, *MNRAS*, **438**, L11
- Binks, A. S., & Jeffries, R. D. 2016, *MNRAS*, **455**, 3345
- Bochanski, J. J., Faherty, J. K., Gagné, J., et al. 2018, *AJ*, **155**, 149
- Boucher, A., Lafrenière, D., Gagné, J., et al. 2016, *ApJ*, **832**, 50
- Buder, S., Sharma, S., Kos, J., et al. 2021, *MNRAS*, **506**, 150
- Chen, C. H., Mittal, T., Kuchner, M., et al. 2014, *ApJS*, **211**, 25
- Coleman, G. A. L., & Haworth, T. J. 2020, *MNRAS*, **496**, L111
- Čotar, K., Zwitter, T., Traven, G., et al. 2021, *MNRAS*, **500**, 4849
- Cotten, T. H., & Song, I. 2016, *ApJSS*, **225**, 15
- Crundall, T. D., Ireland, M. J., Krumholz, M. R., et al. 2019, *MNRAS*, **489**, 3625
- Cruz-Saenz de Miera, F., Chavez, M., Bertone, E., & Vega, O. 2014, *MNRAS*, **437**, 391
- da Silva, L., Torres, C. A. O., de La Reza, R., et al. 2009, *A&A*, **508**, 833
- David, T. J., & Hillenbrand, L. A. 2015, *ApJ*, **804**, 146
- Debes, J. H., Thévenot, M., Kuchner, M. J., et al. 2019, *ApJL*, **872**, L25
- Debes, J. H., Weinberger, A. J., & Song, I. 2008, *ApJL*, **684**, L41
- Dennihey, E., Farihi, J., Fusillo, N. P. G., & Debes, J. H. 2020, *ApJ*, **891**, 97
- Elliott, P., Bayo, A., Melo, C. H. F., et al. 2016, *A&A*, **590**, A13
- Engler, N., Boccaletti, A., Schmid, H. M., et al. 2019, *A&A*, **622**, A192
- Esplin, T. L., Luhman, K. L., Miller, E. B., & Mamajek, E. E. 2018, *AJ*, **156**, 75
- Esposito, T. M., Duchêne, G., Kalas, P., et al. 2018, *AJ*, **156**, 47
- Esposito, T. M., Kalas, P., Fitzgerald, M. P., et al. 2020, *AJ*, **160**, 24
- Faherty, J. K., Bochanski, J. J., Gagné, J., et al. 2018, *ApJ*, **863**, 91
- Fitzpatrick, E. L. 1999, *PASP*, **111**, 63
- Foreman-Mackey, D., Conley, A., Meierjurgen Farr, W., et al. 2013, emcee: The MCMC Hammer, Astrophysics Source Code Library, ascl:1303.002
- Gaia Collaboration, Brown, A. G. A., Vallenari, A., et al. 2018, *A&A*, **616**, A1
- Gagné, J., & Faherty, J. K. 2018, *ApJ*, **862**, 138
- Gagné, J., Faherty, J. K., Moranta, L., & Popinchalk, M. 2021, *ApJL*, **915**, L29
- Gagné, J., Fontaine, G., Simon, A., & Faherty, J. K. 2018a, *ApJL*, **861**, L13
- Gagné, J., Mamajek, E. E., Malo, L., et al. 2018b, *ApJ*, **856**, 23
- Gagné, J., Roy-Loubier, O., Faherty, J. K., Doyon, R., & Malo, L. 2018c, *ApJ*, **860**, 43
- Goldman, B., Röser, S., Schilbach, E., Moór, A. C., & Henning, T. 2018, *ApJ*, **868**, 32
- Grady, C. A., Wisniewski, J. P., Schneider, G., et al. 2020, *ApJL*, **889**, L21
- Guillout, P., Kluttsch, A., Frasca, A., et al. 2009, *A&A*, **504**, 829
- Haakonsen, C. B., & Rutledge, R. E. 2009, *ApJS*, **184**, 138
- Hinkley, S., Matthews, E. C., Lefevre, C., et al. 2021, *ApJ*, **912**, 115
- Holland, W. S., Matthews, B. C., Kennedy, G. M., et al. 2017, *MNRAS*, **470**, 3606
- Indebetouw, R., Mathis, J. S., Babler, B. L., et al. 2005, *ApJ*, **619**, 931
- Kalas, P., Fitzgerald, M. P., & Graham, J. R. 2007, *ApJ*, **661**, L85
- Kastner, J. H. 2016, in *IAU Symp. 314, Young Stars & Planets Near the Sun*, ed. J. H. Kastner, B. Stelzer, & S. A. Metchev (Cambridge: Cambridge Univ. Press), 16
- Kennedy, G. M., & Wyatt, M. C. 2012, *MNRAS*, **426**, 91
- Kounkel, M., & Covey, K. 2019, *AJ*, **158**, 122
- Kral, Q., Matrà, L., Wyatt, M. C., & Kennedy, G. M. 2017, *MNRAS*, **469**, 521
- Kuchner, M. J., Silverberg, S. M., Bans, A. S., et al. 2016, *ApJ*, **830**, 84
- Lambert, T. S., Kraan-Korteweg, R. C., Jarrett, T. H., & Macri, L. M. 2020, *MNRAS*, **497**, 2954
- Lawson, K., Currie, T., Wisniewski, J. P., et al. 2020, *AJ*, **160**, 163
- Lazzoni, C., Desidera, S., Marzari, F., et al. 2018, *A&A*, **611**, A43
- Lee, J., & Song, I. 2019a, *MNRAS*, **486**, 3434
- Lee, J., & Song, I. 2019b, *MNRAS*, **489**, 2189
- Lee, J., Song, I., & Murphy, S. 2020, *MNRAS*, **494**, 62
- Lee, K.-G., Krolewski, A., White, M., et al. 2018, *ApJS*, **237**, 31
- Liu, Q. 2021, *RAA*, **21**, 060
- Luhman, K. L., & Esplin, T. L. 2020, *AJ*, **160**, 44
- MacGregor, M. A., Weinberger, A. J., Nesvold, E. R., et al. 2019, *ApJL*, **877**, L32
- Malo, L., Doyon, R., Lafrenière, D., et al. 2013, *ApJ*, **762**, 88
- Mamajek, E. E. 2009, in *AIP Conf. Ser. 1158, American Institute of Physics Conference Series*, ed. T. Usuda, M. Tamura, & M. Ishii (Melville, NY: AIP), 3
- Mamajek, E. E. 2016, in *IAU Symp. 314, Young Stars & Planets Near the Sun*, ed. J. H. Kastner, B. Stelzer, & S. A. Metchev (Cambridge: Cambridge Univ. Press), 21
- Mamajek, E. E., & Bell, C. P. M. 2014, *MNRAS*, **445**, 2169
- Marigo, P., Girardi, L., Bressan, A., et al. 2017, *ApJ*, **835**, 77
- Mazoyer, J., Boccaletti, A., Augereau, J. C., et al. 2014, *A&A*, **569**, A29
- Melis, C., Zuckerman, B., Rhee, J. H., et al. 2012, *Natur*, **487**, 74
- Melton, E. 2020, *AJ*, **159**, 200
- Meng, H. Y. A., Rieke, G. H., Su, K. Y. L., et al. 2012, *ApJL*, **751**, L17
- Meng, H. Y. A., Rieke, G. H., Su, K. Y. L., & Gáspár, A. 2017, *ApJ*, **836**, 34
- Meng, H. Y. A., Su, K. Y. L., Rieke, G. H., et al. 2015, *ApJ*, **805**, 77
- Meshkat, T., Mawet, D., Bryan, M. L., et al. 2017, *AJ*, **154**, 245
- Messina, S., Lanzafame, A. C., Feiden, G. A., et al. 2016, *A&A*, **596**, A29
- Miret-Roig, N., Galli, P. A. B., Brandner, W., et al. 2020, *A&A*, **642**, A179
- Mittal, T., Chen, C. H., Jang-Condell, H., et al. 2015, *ApJ*, **798**, 87
- Moór, A., Kóspál, Á., Ábrahám, P., et al. 2016, *ApJ*, **826**, 123
- Moór, A., Ábrahám, P., Deras, A., et al. 2006, *ApJ*, **644**, 525
- Moór, A., Ábrahám, P., Szabó, G., et al. 2021, *ApJ*, **910**, 27
- Moór, A., Pascucci, I., Kóspál, Á., et al. 2011, *ApJS*, **193**, 4
- Moór, A., Pawellek, N., Ábrahám, P., et al. 2020, *ApJ*, **154**, 288
- Murphy, S. J., Mamajek, E. E., & Bell, C. P. M. 2018, *MNRAS*, **476**, 3290
- Nesvold, E. R., & Kuchner, M. J. 2015a, *ApJ*, **798**, 83
- Nesvold, E. R., & Kuchner, M. J. 2015b, *ApJ*, **815**, 61
- Nordström, B., Mayor, M., Andersen, J., et al. 2004, *A&A*, **418**, 989
- Oh, S., Price-Whelan, A. M., Hogg, D. W., Morton, T. D., & Spergel, D. N. 2017, *AJ*, **153**, 257
- Ochsenbein, F., Bauer, P., & Marcout, J. 2000, *A&AS*, **143**, 23
- Patel, R. I., Metchev, S. A., & Heinze, A. 2014, *ApJSS*, **212**, 10
- Pawellek, N., Wyatt, M., Matrà, L., Kennedy, G., & Yelverton, B. 2021, *MNRAS*, **502**, 5390
- Pecaut, M. J., & Mamajek, E. E. 2016, *MNRAS*, **461**, 794
- Rhee, J. H., Song, I., Zuckerman, B., & McElwain, M. 2007, *ApJ*, **660**, 1556
- Riedel, A. R., Alam, M. K., Rice, E. L., Cruz, K. L., & Henry, T. J. 2017a, *ApJ*, **840**, 87
- Riedel, A. R., Blunt, S. C., Lambrides, E. L., et al. 2017b, *AJ*, **153**, 95
- Riviere-Marichalar, P., Merín, B., Kamp, I., Eiroa, C., & Montesinos, B. 2016, *A&A*, **594**, A59
- Rodigas, T. J., Hinz, P. M., Leisenring, J., et al. 2012, *ApJ*, **752**, 57
- Romano, D., Burton, M. G., Ashley, M. C. B., et al. 2019, *MNRAS*, **484**, 2089
- Schneider, A., Song, I., Melis, C., et al. 2013, *ApJ*, **777**, 78
- Schneider, A. C., Shkolnik, E. L., Allers, K. N., et al. 2019, *AJ*, **157**, 234
- Schutte, M. C., Lawson, K., Wisniewski, J., et al. 2020, *ApJ*, **160**, 156
- Silverberg, S. M., Kuchner, M. J., Wisniewski, J. P., et al. 2016, *ApJL*, **830**, L28
- Silverberg, S. M., Kuchner, M. J., Wisniewski, J. P., et al. 2018, *ApJ*, **868**, 43
- Silverberg, S. M., Wisniewski, J. P., Kuchner, M. J., et al. 2020, *ApJ*, **890**, 106
- Silverstone, M. D. 2000, PhD thesis, Univ. of California, LOS Angeles
- Soumer, R., Perrin, M. D., Pueyo, L., et al. 2014, *ApJL*, **786**, L23
- Su, K. Y. L., Jackson, A. P., Gáspár, A., et al. 2019, *AJ*, **157**, 202
- Szegedy, C., Liu, W., Jia, Y., et al. 2014, arXiv:1409.4842
- Taylor, M. B. 2005, in *ASP Conf. Ser. 347, Astronomical Data Analysis Software and Systems XIV*, ed. P. Shopbell, M. Britton, & R. Ebert (San Francisco, CA: ASP), 29
- Torres, C. A. O., da Silva, L., Quast, G. R., de la Reza, R., & Jilinski, E. 2000, *AJ*, **120**, 1410
- Torres, C. A. O., Quast, G. R., da Silva, L., et al. 2006, *A&A*, **460**, 695

- Torres, C. A. O., Quast, G. R., Melo, C. H. F., & Sterzik, M. F. 2008, in Handbook of Star Forming Regions, Volume II: The Southern Sky ASP Monograph Publications, ed. B. Reipurth, Vol. 5 (San Francisco, CA: ASP), 757
- Vigan, A., Bonavita, M., Biller, B., et al. 2017, *A&A*, 603, A3
- Wilhelm, M. J. C., & Portegies Zwart, S. 2022, *MNRAS*, 509, 44
- Wu, C.-J., Wu, H., Lam, M.-I., et al. 2013, *ApJSS*, 208, 29
- Zuckerman, B. 2015, *ApJ*, 798, 86
- Zuckerman, B. 2019, *ApJ*, 870, 27
- Zuckerman, B., Klein, B., & Kastner, J. 2019, *ApJ*, 887, 87
- Zuckerman, B., Rhee, J. H., Song, I., & Bessell, M. S. 2011, *ApJ*, 732, 61
- Zuckerman, B., Song, I., & Bessell, M. S. 2004, *ApJL*, 613, L65
- Zuckerman, B., Song, I., Bessell, M. S., & Webb, R. A. 2001a, *ApJL*, 562, L87
- Zuckerman, B., Song, I., & Webb, R. A. 2001b, *ApJ*, 559, 388
- Zuckerman, B., Vican, L., Song, I., & Schneider, A. 2013, *ApJ*, 778, 5